NASA TECHNICAL REPORT

NASA TR R-345

NASA TR R-345

ON THE INFERENCE OF THE PHYSICAL PROPERTIES OF THE JOVIAN ATMOSPHERE FROM PHOTOMETRY OF ECLIPSES OF THE GALILEAN SATELLITES

by Michael J. Price

Goddard Space Flight Center
Greenbelt, Md. 20771

NATIONAL AERONAUTICS AND SPACE ADMINISTRATION • WASHINGTON, D. C. • SEPTEMBER 1970

1. Report No.	2. Government Accession No.	3. Recipient's Catalog No.
NASA TR R-345		

4. Title and Subtitle	5. Report Date
On the Inference of the Physical Properties of the Jovian Atmosphere from Photometry of Eclipses of the Galilean Satellites	September 1970
	6. Performing Organization Code
7. Author(s)	8. Performing Organization Report No.
Michael J. Price	
9. Performing Organization Name and Address	10. Work Unit No.
Goddard Space Flight Center Greenbelt, Maryland 20771	11. Contract or Grant No.
	13. Type of Report and Period Covered
12. Sponsoring Agency Name and Address	Technical Report
National Aeronautics and Space Administration Washington, D.C.	14. Sponsoring Agency Code

15. Supplementary Notes

Researched during the tenure of an NRC-NAS postdoctoral resident research associateship at the Institute for Space Studies.

16. Abstract

The frequent eclipses of the Galilean satellites provide an extremely simple yet extremely powerful method for monitoring the physical structure of the Jovian atmosphere in time, latitude, and longtitude. In this paper, all theoretical and observational problems involved in the use of these eclipses to scan the Jovian atmosphere are discussed in detail. It is shown that a rather complete knowledge of the structure of the Jovian atmosphere immediately above the cloud layer may be obtained from multicolor photometry of the refraction tails of the ingress light curves of the satellites. The relevant observational data may be obtained readily using currently available ground-based astronomical equipment. This technique for inferring the physical structure of a planetary atmosphere may be applied to Saturn also. In that case, the relatively infrequent eclipses of Titan may be utilized.

17. Key Words Suggested by Author	18. Distribution Statement
Galilean satellites Jovian atmosphere Jupiter	Unclassified—Unlimited

19. Security Classif. (of this report)	20. Security Classif. (of this page)	21. No. of Pages	22. Price*
Unclassified	Unclassified	57	$3.00

*For sale by the Clearinghouse for Federal Scientific and Technical Information
Springfield, Virginia 22151

CONTENTS

ON THE INFERENCE OF THE PHYSICAL PROPERTIES OF THE JOVIAN ATMOSPHERE FROM PHOTOMETRY OF ECLIPSES OF THE GALILEAN SATELLITES*

by

Michael J. Price

Goddard Space Flight Center

CHAPTER I

INTRODUCTION

Over 20 years ago Kuiper (1947), reporting visual observations of the integrated brightnesses of Io and Europa as they entered eclipse, called attention to the existence of a tail on each light curve near the 14th magnitude. Kuiper tentatively attributed these tails to refraction in the Jovian atmosphere. This conclusion prompted the first accurate photoelectric photometry of the eclipses of the Galilean satellites, which were made by Kuiper in 1950 and by Kuiper and Harris in 1954. These observations and their interpretation have been discussed in detail by Harris (1961).

From their observations, Kuiper and Harris attempted to determine the refraction properties of the Jovian atmosphere to infer its physical structure. Severe difficulties were encountered, however, in the interpretation of the data. Uncertainties in the radii of the satellites and in the distribution of reflectivity over their disks made the analysis arbitrary. Largely because of these difficulties, no further attempts have been made to use eclipses of the Galilean satellites to probe the Jovian atmosphere.

In this paper the problem of inferring the physical properties of the Jovian atmosphere from photometric observations of the eclipses of the Galilean satellites is thoroughly discussed. All the theoretical and observational problems involved are examined in detail. It is shown that the difficulties encountered by Kuiper and Harris disappear if the photometry is extended to lower light levels. In fact, the satellite eclipses provide a simple and effective means of scanning the Jovian atmosphere to determine its physical properties as functions of height, latitude, longitude, and time.

*Researched during the tenure of an NRC-NAS postdoctoral resident research associateship at the Institute for Space Studies.

CHAPTER 2

JUPITER AND THE GALILEAN SATELLITE SYSTEM

A. Physical Parameters: Mean Satellite

The basic physical parameters of Jupiter and the Galilean satellite system are listed in Tables 2.1 and 2.2, respectively. These data have been obtained from Allen (1963) and Melbourne et al. (1968).

Table 2.1 — Physical parameters of Jupiter and its orbit.

Parameter	Value
Equatorial radius of planet	71,350 km
Ellipticity of planet	0.062
Inclination of plane of equator to plane of orbit	3°05'
Surface gravity (attractive)	2600 cm sec^{-2}
Surface gravity (equator; centrifugal)	-225 cm sec^{-2}
Semimajor axis of orbit	5.2028 AU
Sidereal period	11.86223 tropical years
Synodic period	398.88 days
Eccentricity of orbit	0.048
Mean daily motion	299".1278
Mean orbital velocity	13.06 km/sec
Inclination of orbit to ecliptic	1°18'
Angular diameter of Sun observed from orbit of Jupiter (distance from Sun: 5.2028 AU)	368".9

To facilitate demonstration of the eclipse technique for inferring the physical properties of the Jovian atmosphere, it was decided to use a fictitious mean satellite rather than treat each satellite individually. The physical parameters of this satellite (Table 2.3) are the averaged parameters of the four Galilean satellites. Note that the mean satellite is assumed to revolve around Jupiter in a circular orbit exactly in its equatorial plane, to be spherical, and to have uniform reflectivity over its apparent disk. In addition, because the difference between the sidereal and synodic periods is negligible, it is neglected in the subsequent discussion. For convenience, certain simplifying assumptions

are made concerning Jupiter itself. The planet is assumed to be spherical and to revolve around the Sun in a circular orbit in the plane of the ecliptic.

Table 2.2 — Physical parameters of the Galilean satellites.

	Satellite number			
	I (Io)	II (Europa)	III (Ganymede)	IV (Callisto)
Distance from center of Jupiter (km)	4.22×10^5	6.71×10^5	1.070×10^6	1.883×10^6
Sidereal period (days)	1.769138	3.551181	7.154553	16.689018
Inclination of plane of orbit to Jovian equator (deg)	0	0	0	0
Eccentricity of orbit	0	.0003	.0015	.0075
Mean orbital velocity (km/sec)	17.35	13.71	10.88	8.22
Radius of satellite (km)	1670	1460	2550	2360
Apparent visual magnitude, m_v, at mean opposition	+5.5	+5.8	+5.1	+6.3

Table 2.3 — Physical parameters of fictitious satellite.

Parameter	Value
Distance from center of Jupiter (km)	1.012×10^6
Sidereal period (days)	6.577
Inclination of plane of orbit to Jovian equator (deg)	0
Eccentricity of orbit	0
Mean orbital velocity (km/sec)	11.19
Radius of satellite (km)	2010
Apparent visual magnitude, m_v, at mean opposition	+5.54

B. Eclipses of the Satellites: Basic Geometry

The geometry of an eclipse of the mean satellite is shown in Figures 2.1, 2.2, and 2.3. Because the ingress light curve is far more easily observed than the egress light curve, the discussion will be restricted to the ingress region of the orbit of the satellite.

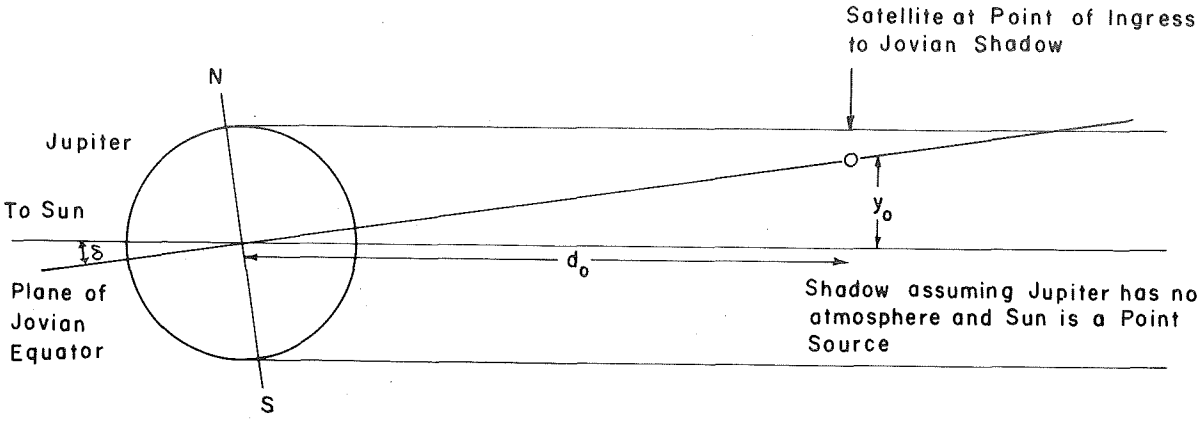

Figure 2.1—Geometry of an eclipse of the mean satellite. The section shown is that through both the center of the Sun and the center of Jupiter, perpendicular to the plane of the Jovian orbit. For simplicity, the special case in which the Jovian polar axis *NS* lies in the plane of the section is shown. In this case, the angle δ is equal to the angle η, the inclination of the Jovian equator to the plane of the Jovian orbit. In the general case, the angle δ is equal to $\eta \cos (l-l_0)$, where l is the mean anomaly of the planet, and l_0 is the corresponding mean anomaly when the north pole of Jupiter is tilted at its greatest angle toward the Sun. The diagram is not to scale.

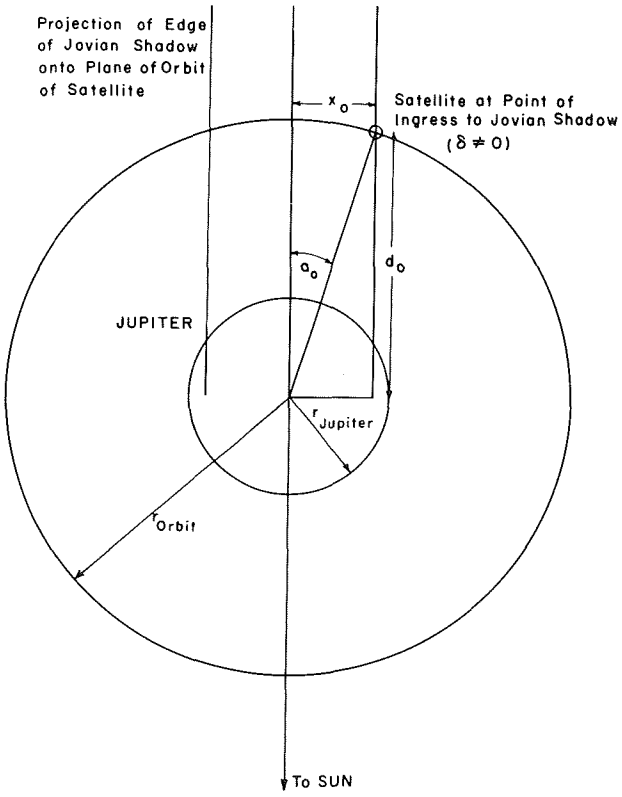

Figure 2.2—Geometry of an eclipse of the mean satellite. The eclipse shown in Figure 2.1 is viewed perpendicular to the plane of the orbit of the satellite. The diagram is not to scale.

To study the effect of refraction by the Jovian atmosphere on the ingress light curve, it is necessary to be able to calculate, for any chosen instant during ingress, the perpendicular distance p from the center of the satellite to the edge of the Jovian shadow. The sharp edge, used for reference, would be produced if the planet had no atmosphere and the Sun were reduced to a point source. With reference to Figure 2.3, the coordinates (x, y) of the center of the satellite must be defined as a function of time t. Time is measured from the instant $(t = 0)$ the center of the satellite is on the reference edge of the shadow at coordinates x_0, y_0. If $r < r_S$, time is counted as positive; if $r > r_S$, time is counted as negative. The quantity r is the distance from the center of the satellite to the center of the Jovian shadow when the satellite is at a distance d_0 from the limb of Jupiter. The quantity r_S is the radius of the point-source geometrical shadow of the planet at the same distance from the limb. The quantity d_0 is the distance from the center of the satellite to the limb of

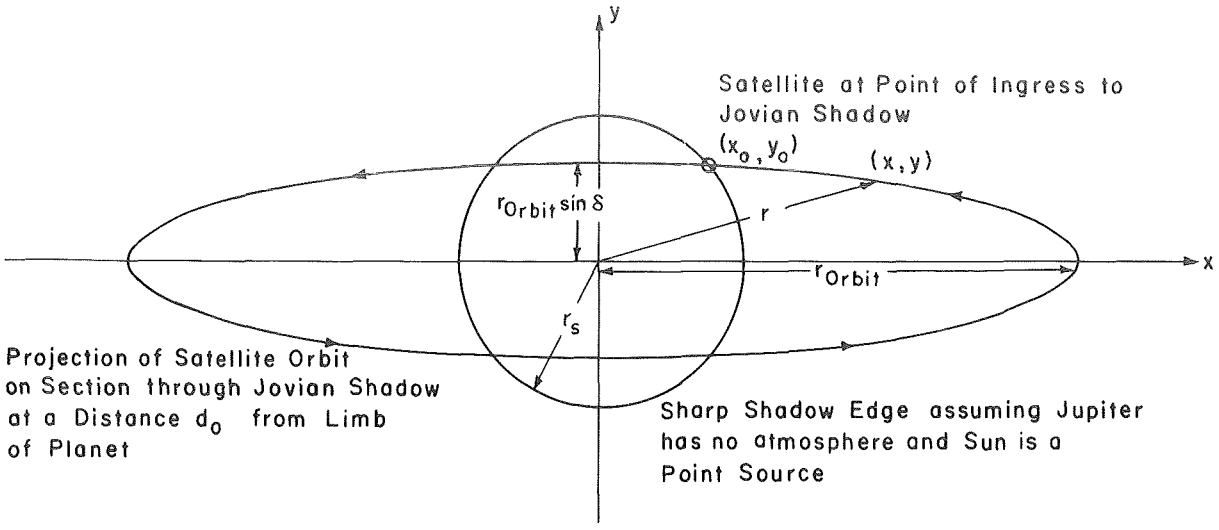

Figure 2.3—Geometry of an eclipse of the mean satellite. The eclipse shown in Figure 2.1 is viewed here from the center of Jupiter along the prolonged radius vector from the Sun. The section is taken perpendicular to the axis of the shadow at a distance d_0 from the center of Jupiter. The diagram is not to scale.

Jupiter at ingress, measured along the length of the shadow. To a good approximation we can assume that d_0 is equal to r_{orbit}, the radius of the orbit of the satellite. This assumption is weakest when r_{orbit} is small. However, even for Jupiter I the error in d_0 is never greater than 2 percent, and the approximation is, therefore, adequate for our discussion.

The quantity p at any chosen instant is given by

$$p = r_s - \sqrt{x^2 + y^2}, \tag{2.1}$$

where x, y are the coordinates of the center of the satellite at time t. The quantity r_s is given by

$$r_s = r_{\text{Jupiter}} \left[1 + \frac{d_0}{R_{\text{Jupiter}}} \right], \tag{2.2}$$

where r_{Jupiter} is the radius of Jupiter and R_{Jupiter} is the distance of Jupiter from the Sun. We assume that d_0 is constant for the duration of the ingress light curve. The corresponding uncertainty in the determination of r_s never exceeds 5 parts in 10^4.

The equation for the reference edge of the Jovian shadow is

$$x^2 + y^2 = r_s^2, \tag{2.3}$$

and the equation for the orbit of the satellite, projected on the (x, y) plane, is

$$x^2 + \frac{y^2}{\sin^2 \delta} = r_{orbit}^2 . \tag{2.4}$$

The angle δ is defined as

$$\delta = \eta \cos (l - l_0) , \tag{2.5}$$

where

- η is the inclination of the Jovian equator to the plane of the Jovian orbit
- l is the mean anomaly of the planet
- l_0 is the corresponding mean anomaly when the north pole of Jupiter is tilted at its greatest angle toward the Sun.

The coordinates (x_0, y_0) may be obtained by solving Equations 2.3 and 2.4 simultaneously.

The coordinates (x, y) at any time t during ingress may be calculated in the following manner. With reference to Figure 2.2, the angle α_0 is defined such that

$$\alpha_0 = \sin^{-1}\left[\frac{x_0}{r_{orbit}}\right] \tag{2.6}$$

We define another angle, α_1, such that

$$\alpha_1 = - \nu t, \tag{2.7}$$

where υ is the mean orbital velocity of the satellite. If we write

$$\alpha = \alpha_0 + \alpha_1 , \tag{2.8}$$

it follows that

$$x = r_{orbit} \sin \alpha. \tag{2.9}$$

It then follows from Equation 2.4 that

$$y = \sqrt{r_{orbit}^2 - x^2} \sin \delta . \tag{2.10}$$

Eclipses of the Galilean satellites occur very frequently. For Jupiter I, II, and III, an eclipse always occurs during each revolution of the satellite around the planet. In the case of Jupiter IV, however, an eclipse does not occur under all circumstances. During the course of the Jovian year, the planetocentric declination of the Sun varies between $\pm 3^\circ 05'$, depending on how much the polar axis is tilted toward or away from the Sun. The planetocentric declination of the Sun depends on the location of the planet in its orbit since the direction of the polar axis is very nearly fixed in space. The large distance of

Jupiter IV from the center of the planet prevents the occurrence of eclipses during two periods when the planetocentric declination of the Sun is either more northerly or more southerly than $2^\circ 10'$. In the former case, Jupiter IV passes north of the shadow; in the latter case, it passes to the south. Eclipses of the other three satellites continue to occur during both these periods because their distances from the center of Jupiter are much smaller.

At all points in the Jovian orbit, eclipses occur so frequently that scarcely a day goes by on Earth when one or more does not occur. The eclipses are fairly uniformly distributed in time, largely because of a particular relation that exists between the motions of Jupiter I, II, and III. This relation is exact and permanent and can be shown mathematically to be a necessary consequence of the mutual gravitational perturbations between the three satellites. If θ_1, θ_2, and θ_3 are the mean longitudes of the satellites in their orbits, measured from some initial radius through the center of Jupiter, then

$$\theta_1 + 2\theta_3 - 3\theta_2 = 180^\circ. \tag{2.11}$$

This relation ensures that all three satellites can never exhibit the same phenomena at the same time. Because observations of the eclipses can be made throughout the Jovian orbital period, it is possible to monitor the physical structure of its atmosphere quite thoroughly in time. Diurnal variation of the atmosphere may also be monitored in a crude fashion. The ingress light curves contain information concerning the physical structure of the atmosphere at dusk; the egress light curves contain the corresponding information at dawn.

Variation in the physical structure of the atmosphere in both latitude and longitude may also be monitored. The atmospheric structure may be scanned quite uniformly in longitude since the rotation period of Jupiter is uncorrelated with the orbital periods of the satellites. Consequently, each ingress light curve contains information concerning the atmosphere at a different longitude. The variation in the planetocentric declination of the Sun during the orbital period, caused by the Jovian polar axis not being perpendicular to the plane of the Jovian orbit, permits the atmospheric structure to be scanned completely in latitude twice during the same period. Reference to Figure 2.1 and Tables 2.1 and 2.2, together with the application of simple geometry, shows that the ranges of latitude scanned by the four satellites during the Jovian orbital period are $\pm 18^\circ 30'$ by Jupiter I, $\pm 30^\circ 18'$ by Jupiter II, $\pm 53^\circ 37'$ by Jupiter III, and $\pm 90^\circ 00'$ by Jupiter IV.

The duration of ingress increases as the absolute value of the planetocentric declination of the Sun increases, while the total duration of the eclipse from ingress to egress decreases. Reference to Figure 2.3 shows that the satellite strikes the edge of the shadow at a progressively shallower angle as x_0 decreases and y_0 increases. In particular, Jupiter IV can strike the shadow at any angle from normal to tangential.

To simplify the treatment of the geometry of the eclipse as far as possible in the subsequent discussion, it will be assumed that the angle δ is equal to zero so that at ingress the satellite intersects the shadow along the direction of the normal. It follows that (Figure 2.3) the projected satellite orbit will be reduced to a straight line since the plane of the orbit then contains the line of sight from Earth.

CHAPTER 3

THEORY OF A SATELLITE ECLIPSE: INGRESS LIGHT CURVE

A. Introductory Remarks

Before discussing the theory of the ingress light curve in detail, it will be helpful to describe briefly the view of the Sun and Jupiter as seen by an observer situated on one of the Galilean satellites as it enters the Jovian shadow. If Jupiter had no atmosphere above its cloud level, light from the limb of the Sun that was apparently closest to the planetary limb would be progressively occulted by the clouds as the satellite gradually entered the shadow. At any point during ingress, the Sun would appear as a truncated disk. Eventually, the entire disk would be occulted, and no sunlight would reach the satellite until it began to leave the shadow at egress. In reality, of course, Jupiter has a substantial gaseous atmosphere above its cloud tops that will strongly influence the nature of the solar eclipse phenomena seen by an observer on the satellite. First, the apparent occultation of the solar disk will be delayed by refraction of the sunlight in the atmosphere above the clouds. Second, the shape of the refracted solar disk, and its apparent brightness, will be strongly affected by differential refraction. The refracted solar disk will appear compressed in a direction perpendicular to the limb of the planet, and its brightness will be reduced. Third, both the apparent brightness and color of the refracted solar disk will be affected by scattering. If the atmosphere above the clouds is clear and gaseous, Rayleigh scattering will both redden the solar disk and reduce its intensity. If the atmosphere is not perfectly clear, but contains in addition a haze of cloud particles, further extinction of light and modification of its color will result from scattering by aerosols. Fourth, throughout the eclipse, the atmosphere of Jupiter above the cloud tops will be visible to the observer as a narrow bright ring because of multiple scattering of sunlight in the illuminated hemisphere. To the observer, the disappearance of the Sun behind the limb of the planet will be quite similar to a sunset on Earth as seen from a manned spacecraft in near-Earth orbit. The appearance of the solar disk will be the same whether the light rays are prevented from reaching the observer by their inability to penetrate the thick cloud layer or by critical refraction occurring at some height above the cloud tops.

We will discuss here only the illumination of the satellite by either the unrefracted or refracted solar disk. The possible effects on the ingress light curve of haziness in the atmosphere above an ill-defined cloud level and the bright atmospheric ring surrounding the planet will be discussed later in the paper. For simplicity, we will assume that the

atmosphere above the cloud tops is perfectly clear and gaseous, that the cloud tops are at a very sharply defined level in the Jovian atmosphere, and that the clouds themselves are completely opaque.

B. Standard Model of Jovian Atmosphere

A knowledge of the physical properties of the gaseous atmosphere above the cloud tops is essential for determining quantitatively the effect of the atmospheric refraction on the ingress light curve for the mean satellite. Such information has been obtained primarily by spectroscopy.

Recently, Fink and Belton (1969) analyzed three of the H_2 quadrupole lines in the spectrum of Jupiter, viz. the 3-0 S(0), the 3-0 S(1), and the 4-0 S(1) lines. A reflecting layer model was used in their interpretation to obtain both an abundance of H_2 and a mean temperature for the atmosphere above an effective level of reflection. Their analysis gave an H_2 abundance of 67 $\pm$17 km atm above the clouds, and a mean temperature of 145° $\pm$20°K. Their work was an extension of that by Owen and Mason (1968) who also analyzed two of the H_2 quadrupole lines, viz. the 3-0 S(1) and the 4-0 S(1) lines. They derived the abundance of H_2 above the clouds for each line in turn with the aid of a reflecting layer model. The results for both lines were consistent. The 3-0 S(1) line gave an H_2 abundance of 85 $\pm$15 km atm; the 4-0 S(1) line gave 90 $\pm$17 km atm.

Owen and Mason discussed the problem of the relative abundance of the elements in the Jovian atmosphere. Evidence was presented to indicate that the abundances are similar to those in the Sun. Molecular hydrogen appears to be the major constituent of the atmosphere. An analysis of the collisional broadening of lines in the methane bands in the Jovian spectrum shows that the line widths are consistent with an essentially pure H_2 atmosphere. There remains, however, a small discrepancy between the theoretical and observed line widths, the theoretical width being smaller. This discrepancy may be removed by including some helium with H_2 in the collisional broadening theory. The maximum amount of helium above the clouds, consistent with the observed line widths, is 13 km atm. In that case the H_2/He ratio is $\sim$7. The corresponding H/He ratio for the Sun, given by Biswas and Fichtel (1965), is $\sim$ 11, with a large uncertainty. Methane and ammonia, the only gases besides H_2 detected in the Jovian atmosphere, are very minor constituents by numbers.

In application of the theory of the ingress light curve, a standard model will be used to describe the atmosphere above the clouds. The effects of variation in the standard model will also be studied. The basic assumptions made for each model will be that the atmosphere is spherically symmetric, in hydrostatic equilibrium, homogeneous, isothermal, and composed only of hydrogen and helium. The parameters of the standard model are based on the results obtained by Fink and Belton (1969). The temperature T of the atmosphere will be assumed to be 145°K, and the H_2/He ratio by numbers will be taken as 5.1. The total pressure P_0 at the cloud tops may be derived if the scale height of the atmosphere is known. For the scale height, we will adopt the value of 8.3 km obtained by Baum and Code (1953) from a stellar occultation. The corresponding value of P_0 will be 5.14×10^6 dynes cm^{-2}. The total particle number density at the surface, N_0, may be readily calculated from P_0 and T. From the ideal gas law we have

$$N_0 = \frac{P_0}{kT} = 2.57 \times 10^{20}\ \mathrm{cm}^{-3}, \tag{3.1}$$

where k is Boltzmann's constant.

C. Optical Parameters of a Gaseous Atmosphere

Refractivity

The standard formula for determining the refractivity of a gas at STP is

$$(n-1)_{\mathrm{STP}} = A\left(1 + \frac{B}{\lambda^2}\right), \tag{3.2}$$

where λ is the wavelength and A and B are constants for the particular gas. Values of A and B were tabulated for H_2 and He by Allen (1963).

The refractivity $[n(r)-1]$ at distance r from the center of the planet is proportional to the number density $N(r)$ of the atoms or molecules responsible for the refraction. It follows, therefore, that

$$[n(r)-1] = \frac{N(r)}{L}(n-1)_{\mathrm{STP}}, \tag{3.3}$$

where L is Loschmidt's number.

Specifically, the refractivity at the cloud tops is

$$[n(r_0)-1] = \frac{N(r_0)}{L}(n-1)_{\mathrm{STP}}. \tag{3.4}$$

Since we know that

$$N(r) = N(r_0)\exp\left(-\frac{h}{H}\right), \tag{3.5}$$

where h, the height above the cloud tops, is given by

$$h = r - r_0, \tag{3.6}$$

r_0 being the distance from the center of the planet to the cloud tops, and H is the scale height of the atmosphere, it follows that

$$[n(r)-1] = [n(r_0)-1]\exp\left(-\frac{h}{H}\right). \tag{3.7}$$

Rayleigh Scattering Cross Section

From Allen (1963), the Rayleigh scattering cross section σ may be written as

$$\sigma = \frac{128\pi^5\alpha^2}{3\lambda^4}, \tag{3.8}$$

where α is the polarizability of the atom or molecule. Allen gives a further formula which relates the polarizability to the refractivity at STP. We have that

$$(n - 1)_{STP} = 1.689 \times 10^{20}\,\alpha. \tag{3.9}$$

It is easy to show with the aid of Equation 3.2 that

$$\sigma = \frac{a_0}{\lambda^4}\left(1 + \frac{a_1}{\lambda^2} + \frac{a_2}{\lambda^4}\right), \tag{3.10}$$

where a_0, a_1, and a_2 are constants, readily calculable for any atom or molecule from the data given by Allen.

Effective Refractivity and Effective Rayleigh Scattering Cross Section

If the gaseous atmosphere above the clouds is composed of several different gases (e.g., H_2 and He), it is necessary to use both an effective refractivity and an effective Rayleigh scattering cross section. If the total number of atoms and molecules per cubic centimeter is written as $N(r)_{total}$, then

$$N(r)_{total} = N(r)_{H_2} + N(r)_{He}, \tag{3.11}$$

where $N(r)_{H_2}$ and $N(r)_{He}$ are, respectively, the number densities of H_2 and He at the particular point in the atmosphere under consideration. If the effective refractivity is written as $[n(r)-1]_{effective}$, we have

$$[n(r) - 1]_{effective} = f_1(r)\,[n(r) - 1]_{H_2} + f_2(r)\,[n(r) - 1]_{He}. \tag{3.12}$$

The quantities $[n(r)-1]_{H_2}$ and $[n(r)-1]_{He}$ are, respectively, the refractivities of H_2 and He. The refractivities may be calculated with the aid of Equations 3.2 through 3.7. In each equation the number density of atoms or molecules is taken as $N(r)_{total}$. The parameters $f_1(r)$ and $f_2(r)$ are defined by

$$f_1(r) = \frac{N(r)_{H_2}}{N(r)_{H_2} + N(r)_{He}} \tag{3.13}$$

and

$$f_2(r) = \frac{N(r)_{He}}{N(r)_{H_2} + N(r)_{He}}. \tag{3.14}$$

If the ratio $N(r)_{H_2}/N(r)_{He}$ is assumed to be invariant with height in the atmosphere, f_1 and f_2 will be constant with height also. If the effective Rayleigh scattering cross section is written as $\sigma_{effective}$, we have

$$\sigma_{\text{effective}} = f_1 \sigma_{H_2} + f_2 \sigma_{He}, \tag{3.15}$$

where σ_{H_2} and σ_{He} are, respectively, the Rayleigh scattering cross sections for H_2 and He.

D. Refraction Through a Planetary Atmosphere

The effect of refraction on the transmission of light through a planetary atmosphere has been discussed by Pannekoek (1903) and Fabry (1929). Both considered only the special case of the occultation of a star by a planet as observed from Earth. Attention was given to the determination of the angle of refraction, the path length through the atmosphere, and the attenuation by differential refraction. Here the theory of refraction in a planetary atmosphere is given in greater detail. The theory has been generalized to treat the illumination of a finite satellite by light refracted through a planetary atmosphere from a finite solar source.

The problem of determining the path of a ray of light through a planetary atmosphere reduces to finding the curve Γ for which the travel time T is a minimum. The travel time T is defined by

$$T_t = \int^{\Gamma} \frac{ds}{v} = \text{minimum}, \tag{3.16}$$

where ds is an element of path length, and v is the velocity of light in the atmosphere at the corresponding point along the path. The velocity v is given by

$$v = \frac{c}{n}, \tag{3.17}$$

where n is the refractive index, and c is the velocity of light in a vacuum. The model atmosphere adopted for the refraction problem, like the standard model of the Jovian atmosphere, is assumed to be spherically symmetric, homogeneous, in hydrostatic equilibrium, and to have a scale height H constant with altitude in the atmosphere. The refractive index may, therefore, be written as $n(r)$ since it is a function only of the distance from the center of the planet. The element of path length ds may be described by polar coordinates as defined in Figure 3.1. We have

$$ds^2 = (r d\theta)^2 + (dr)^2. \tag{3.18}$$

Equation 3.16 may, therefore, be rewritten as

$$T = \int_a^b \frac{n(r)}{c} \left[r^2 \left(\frac{d\theta}{dr} \right)^2 + 1 \right]^{1/2} dr, \tag{3.19}$$

where a and b represent the limit in r of the curve Γ.

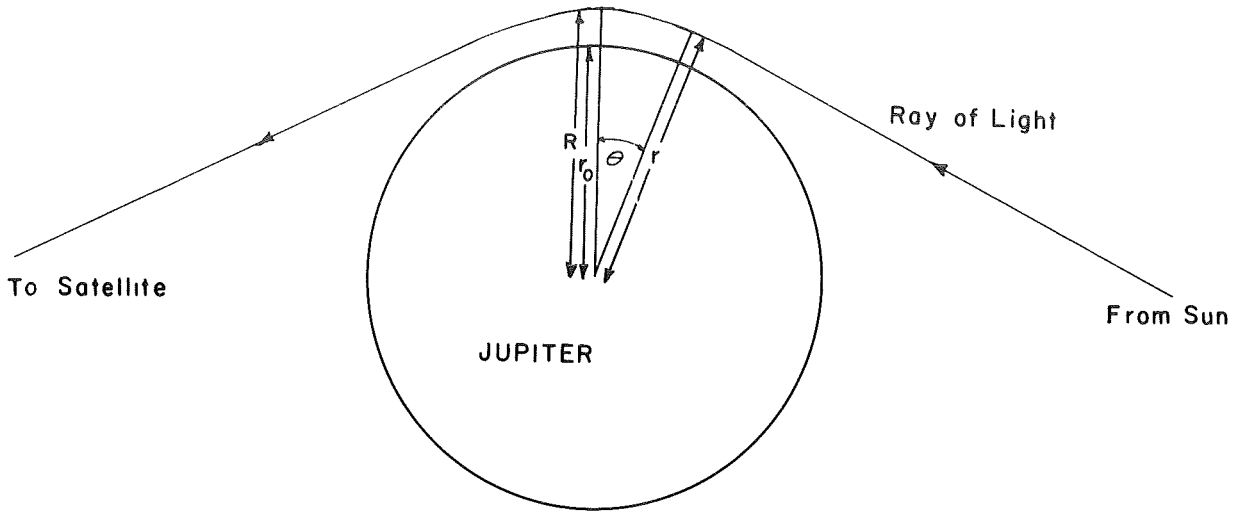

Figure 3.1—Schematic representation of refraction in the Jovian atmosphere.

The integral in Equation 3.19 is of the general form

$$J = \int_a^b \Phi(x,y,y')\,dx, \tag{3.20}$$

where, in the usual notation,

$$y' = \frac{dy}{dx}. \tag{3.21}$$

From the calculus of variations, the Euler-Lagrange differential equation for the extremum of J is

$$\frac{\partial \Phi}{\partial y} - \frac{d}{dx}\left(\frac{\partial \Phi}{\partial y'}\right) = 0. \tag{3.22}$$

The solution, $y = f(x)$, of Equation 3.22 gives the equation of the path Γ_0 in the x, y-plane which makes J an extremum.

Equation 3.19 is of the particular form

$$J = \int_a^b \Phi(x,y')\,dx, \tag{3.23}$$

which results when Φ does not contain y explicitly. In this case the corresponding Euler-Lagrange differential equation is simply

$$\frac{d}{dx}\left(\frac{\partial \Phi}{\partial y'}\right) = 0. \tag{3.24}$$

It follows that the equation whose solution will determine the path of the refracted light ray through the atmosphere is

$$\frac{d}{dr}\left(\frac{\partial f}{\partial \dot{\theta}}\right) = 0, \tag{3.25}$$

where

$$\dot{\theta} = \frac{d\theta}{dr} \tag{3.26}$$

and

$$f = f(r,\dot{\theta}) = \frac{n(r)}{c}\left[r^2\left(\frac{d\theta}{dr}\right)^2 + 1\right]^{1/2}. \tag{3.27}$$

Equation 3.25 then becomes, after multiplying through by c,

$$\frac{d}{dr}\left\{n(r)\left[r^2\left(\frac{d\theta}{dr}\right)^2 + 1\right]^{-1/2} r^2\frac{d\theta}{dr}\right\} = 0. \tag{3.28}$$

If we integrate Equation 3.28 once, use C_1 to represent the constant of integration, and then rearrange the resultant equation, we obtain

$$\frac{d\theta}{dr} = \frac{C_1}{r\left[n^2(r)r^2 - C_1^2\right]^{1/2}}. \tag{3.29}$$

The constant C_1 may be evaluated immediately by noting the end conditions corresponding to a and b, which are the limits in r of the curve. At a, $r = R$, $n(r) = n(R)$, and $\theta = 0$. The quantity R is the distance of closest approach of the refracted light ray to the center of the planet. If the ray of light is to traverse the atmosphere, we must have the condition that

$$R \geqslant r_0, \tag{3.30}$$

where r_0 is the distance either from the cloud tops or from the level of critical refraction, to the center of the planet. If the level of critical refraction is above the clouds, the value of r_0 corresponds to that level; vice versa, the value of r_0 corresponds to the level of the cloud tops. At b, $r = \infty$, $n(r) = 1$, $\theta = \theta_\infty$. It follows that

$$C_1 = n(R)R\,. \tag{3.31}$$

The equation to be integrated, therefore, is

$$\theta_\infty = \int_a^b \frac{n(R)R\,dr}{r[n^2(r)r^2 - n^2(R)R^2]^{1/2}}. \tag{3.32}$$

To solve Equation 3.32, a change in variables is made. Let

$$u = rn(r) = rn$$

$$u_0 = Rn(R)$$

$$du = \left[rn'(r) + n(r) \right] dr = (rn' + n)\, dr, \tag{3.33}$$

where

$$n'(r) = \frac{dn(r)}{dr} = \frac{dn}{dr}.$$

Equation 3.32 may be rewritten as

$$\theta_\infty = \int_{u_0}^{u_1} \frac{nu_0 du}{u(u^2 - u_0^2)^{1/2}(rn' + n)}, \tag{3.34}$$

where u_0 and u_1 correspond to a and b, respectively.

Equation 3.34 becomes

$$\theta_\infty = u_0 \int_{u_0}^{u_1} \left(1 - \frac{rn'/n}{1 + rn'/n}\right) \frac{1}{u(u^2 - u_0^2)^{1/2}}\, du \tag{3.35}$$

or

$$\theta_\infty = u_0 \int_{u_0}^{u_1} \frac{du}{u(u^2 - u_0^2)^{1/2}} - u_0 \int_{u_0}^{u_1} \frac{rn'du}{u(u^2 - u_0^2)^{1/2}\,(n + rn')}. \tag{3.36}$$

If u_1 is replaced by ∞, the first term of Equation 3.36 may be readily integrated. If the variable is changed by making the substitution

$$p^2 = u^2 - u_0^2, \tag{3.37}$$

the integral takes a standard form. Equation 3.36 reduces, therefore, to

$$\theta_\infty = \frac{\pi}{2} - u_0 \int_{u_0}^{\infty} \frac{rn'du}{u(u^2 - u_0^2)^{1/2}\,(n + rn')}. \tag{3.38}$$

The angle of bending η from infinity to the point of closest approach to the center of the planet is given by

$$\eta = -u_0 \int_{u_0}^{\infty} \frac{rn'du}{u(u^2 - u_0^2)^{1/2}\,(n + rn')}. \tag{3.39}$$

The total angle of bending ϵ suffered by the light ray in traversing the entire atmosphere is, therefore, given by

$$\epsilon = 2\eta \tag{3.40}$$

or

$$\epsilon = -2u_0 \int_{u_0}^{\infty} \frac{rn'du}{u(u^2 - u_0^2)^{1/2}\,(n + rn')} . \tag{3.41}$$

Equation 3.41 may be rewritten as

$$\epsilon = -2n(R)R \int_{R}^{\infty} \frac{n'(r)\,dr}{n(r)\left[n^2(r)r^2 - n^2(R)R^2\right]^{1/2}} . \tag{3.42}$$

The refractivity, $[n(r)-1]$, is proportional to the number density $N(r)$ of the refracting particles. It follows that the refractive index $n(r)$ has the form

$$n(r) = \left[n(r_0) - 1\right] \exp\left[-\frac{(r-r_0)}{H}\right] + 1 , \tag{3.43}$$

since

$$N(r) = N(r_0) \exp\left[-\frac{(r - r_0)}{H}\right] . \tag{3.44}$$

Differentiating Equation 3.43 with respect to r we obtain

$$n'(r) = -\frac{1}{H}\left[n(r_0) - 1\right] \exp\left[-\frac{(r - r_0)}{H}\right] . \tag{3.45}$$

For the particular model planetary atmospheres considered in this paper it is always a good approximation to write that

$$n(r) \cong 1 \tag{3.46}$$

and

$$n(r) - 1 << 1 . \tag{3.47}$$

Substituting Equation 3.45 into Equation 3.42 we obtain

$$\epsilon = -2n(R)R \int_{R}^{\infty} \frac{-\frac{1}{H}\left[n(r_0) - 1\right] \exp\left[-\frac{(r - r_0)}{H}\right] dr}{n(r)\left[n^2(r)r^2 - n^2(R)R^2\right]^{1/2}} . \tag{3.48}$$

Therefore,

$$\epsilon = 2n(R)\frac{R}{H}\left[n(r_0) - 1\right] \exp\left(\frac{r_0}{H}\right) \int_{R}^{\infty} \frac{\exp\left(\frac{-r}{H}\right) dr}{n(r)\left[n^2(r)r^2 - n^2(R)R^2\right]^{1/2}} . \tag{3.49}$$

Making use of the approximations in Equations 3.46 and 3.47 we obtain

$$\epsilon = 2\frac{R}{H}\left[n(r_0) - 1\right] \exp\left(\frac{r_0}{H}\right)\int_R^\infty \frac{\exp\left(\frac{-r}{H}\right)dr}{(r^2 - R^2)^{1/2}}. \tag{3.50}$$

To solve the integral in Equation 3.50 we make the substitution

$$t = r - R, \tag{3.51}$$

and obtain

$$\epsilon = 2\left[n(r_0) - 1\right]\frac{R}{H}\exp\left[-\frac{(R - r_0)}{H}\right]\int_0^\infty \frac{\exp\left(\frac{-t}{H}\right)dt}{(t^2 + 2Rt)^{1/2}}. \tag{3.52}$$

If we write

$$h_0 = R - r_0, \tag{3.53}$$

where h_0 is the height of the light ray above the cloud tops at the point of closest approach to the center of the planet, we obtain

$$\epsilon = 2\left[n(r_0) - 1\right]\frac{R}{H}\exp\left(-\frac{h_0}{H}\right)\int_0^\infty \frac{\exp\left(\frac{-t}{H}\right)dt}{(t^2 + 2Rt)^{1/2}}. \tag{3.54}$$

The integral in Equation 3.54 is of standard form and may be obtained from Erdélyi (1953). Equation 3.54 reduces, therefore, to

$$\epsilon = 2\left[n(r_0) - 1\right]\left(\frac{R}{H}\right)\exp\left(\frac{-h_0}{H}\right)K_0\left(\frac{R}{H}\right)\exp\left(\frac{R}{H}\right), \tag{3.55}$$

where $K_0(R/H)$ is one of the modified Bessel functions. From Watson (1958) we know that $K_0(x)$ has the asymptotic expansion

$$\exp(x)\,K_0(x) = \left(\frac{\pi}{2x}\right)^{1/2}\left(1 - \frac{1}{8x} + \frac{9}{2(8x)^2} - \cdots\right). \tag{3.56}$$

For large values of x we can write

$$K_0(x)\exp(x) \cong \left(\frac{\pi}{2x}\right)^{1/2}. \tag{3.57}$$

In the case of refraction in the Jovian atmosphere we know that

$$\frac{R}{H} >> 1. \tag{3.58}$$

It follows, therefore, that Equation 3.55 may be rewritten as

$$\epsilon = 2\left[n(r_0) - 1\right]\frac{R}{H}\exp\left(\frac{-h_0}{H}\right)\left(\frac{\pi H}{2R}\right)^{1/2} \tag{3.59}$$

or

$$\epsilon = \left(\frac{2\pi R}{H}\right)^{1/2}\left[n(r_0) - 1\right]\exp\left(\frac{-h_0}{H}\right). \tag{3.60}$$

Equation 3.60 may be rewritten as

$$\epsilon = \epsilon_0 \exp\left(\frac{-h_0}{H}\right), \tag{3.61}$$

where

$$\epsilon_0 = \left(\frac{2\pi R}{H}\right)^{1/2}\left[n(r_0) - 1\right]. \tag{3.62}$$

E. Critical Refraction in a Planetary Atmosphere

A ray of light being refracted through a planetary atmosphere is moving horizontally, at its point of closest approach, to the center of the planet. Critical refraction occurs when the refractive bending is sufficient to give the light ray a radius of curvature equal to the radius of the surface of constant refractive index that passes through that point in the atmosphere. For the case of a spherically symmetric, gaseous, homogeneous, isothermal planetary atmosphere, it is a simple matter to show from Snell's law of refraction that the radius of curvature R_c of a horizontal ray is given by

$$\frac{1}{R_c} = \left[\frac{n(R) - 1}{n(R)}\right]\left(\frac{1}{H}\right). \tag{3.63}$$

The level in any particular model atmosphere at which a horizontally moving ray of light of a particular wavelength suffers critical refraction can, therefore, be readily determined. Rays of light that remain entirely above that level while traversing the atmosphere cannot suffer critical refraction. However, rays of light that penetrate deeper than the level of critical refraction will be trapped by the atmosphere and totally absorbed.

F. Extinction Along the Path Length of a Ray of Light Traversing a Planetary Atmosphere

The extinction factor for a ray of light being refracted through a planetary atmosphere is $\exp(-N_T\sigma)$, where σ is the effective Rayleigh scattering cross section and N_T is the number of gaseous particles per cm^2 integrated along the path length through the atmosphere. N_T is given by

$$N_T = \int^{\Gamma} N(s)\, ds. \tag{3.64}$$

From Equation 3.18 we have

$$N_T = \int^{\Gamma} N(r) \left[r^2 \left(\frac{d\theta}{dr} \right)^2 + 1 \right]^{1/2} dr. \tag{3.65}$$

From Equation 3.44 we have

$$N_T = 2 \int_R^{\infty} N(r_0) \exp \left[\frac{-(r - r_0)}{H} \right] \left[r^2 \left(\frac{d\theta}{dr} \right)^2 + 1 \right]^{1/2} dr. \tag{3.66}$$

or

$$N_T = 2N(r_0) \exp\left(\frac{r_0}{H} \right) \int_R^{\infty} \exp \left(-\frac{r}{H} \right) \left[r^2 \left(\frac{d\theta}{dr} \right)^2 + 1 \right]^{1/2} dr. \tag{3.67}$$

From Equations 3.29 and 3.31 we have

$$N_T = 2N(r_0) \exp\left(\frac{r_0}{H} \right) \int_R^{\infty} \exp \left(-\frac{r}{H} \right) \left(\frac{n^2(R)R^2}{n^2(r)r^2 - n^2(R)R^2} + 1 \right)^{1/2} dr, \tag{3.68}$$

which becomes

$$N_T = 2N(r_0) \exp\left(\frac{r_0}{H} \right) \int_R^{\infty} \exp \left(-\frac{r}{H} \right) \left(\frac{n^2(r)r^2}{n^2(r)r^2 - n^2(R)R^2} \right)^{1/2} dr. \tag{3.69}$$

By rearranging the integral in Equation 3.69 we obtain

$$N_T = 2N(r_0) \exp\left(\frac{r_0}{H} \right) \int_R^{\infty} \exp \left(-\frac{r}{H} \right) \left(\frac{1}{1 - \dfrac{n^2(R)R^2}{n^2(r)r^2}} \right)^{1/2} dr. \tag{3.70}$$

By making use of the approximations in Equations 3.46 and 3.47,

$$N_T = 2N(r_0) \exp\left(\frac{r_0}{H} \right) \int_R^{\infty} \frac{\exp\left(\dfrac{-r}{H} \right)}{\left(1 - \dfrac{R^2}{r^2} \right)^{1/2}} dr. \tag{3.71}$$

Let

$$r = R + t\,. \tag{3.72}$$

Substituting Equation 3.72 in Equation 3.71 we obtain

$$N_T = 2N(r_0) \exp\left[-\frac{(R - r_0)}{H}\right] \int_0^\infty \frac{(R + t) \exp\left(\frac{-t}{H}\right)}{(t^2 + 2Rt)^{1/2}} dt. \tag{3.73}$$

Therefore,

$$N_T = 2N(r_0) \exp\left(\frac{-h_0}{H}\right) \int_0^\infty \frac{(R + t) \exp\left(\frac{-t}{H}\right)}{(t^2 + 2Rt)^{1/2}} dt. \tag{3.74}$$

The integral in Equation 3.74 may be evaluated readily. It has a standard form and its solution may be obtained from Erdélyi (1953). Equation 3.74 becomes

$$N_T = 2N(r_0) R \exp\left(\frac{-h_0}{H}\right) K_1\left(\frac{R}{H}\right) \exp\left(\frac{R}{H}\right), \tag{3.75}$$

where $K_1 (R/H)$ is one of the modified Bessel functions. From Watson (1958) we know that $K_1 (x)$ has the asymptotic expansion

$$\exp(x) K_1(x) = \left(\frac{\pi}{2x}\right)^{1/2} \left(1 + \frac{3}{8x} - \frac{15}{2(8x)^2} + \cdots\right). \tag{3.76}$$

Since we know that

$$\frac{R}{H} >> 1 \tag{3.77}$$

for the case of refraction in the Jovian atmosphere, it follows that

$$N_T = 2N(r_0) R \exp\left(\frac{-h_0}{H}\right)\left(\frac{\pi H}{2R}\right)^{1/2}, \tag{3.78}$$

which may be rewritten as

$$N_T = (2\pi RH)^{1/2} N(r_0) \exp\left(\frac{-h_0}{H}\right). \tag{3.79}$$

G. Attenuation by Differential Refraction for a Ray of Light Traversing a Planetary Atmosphere

The effect of differential refraction in the Jovian atmosphere on the ingress light curve may be examined with the aid of Figure 3.2. Differential refraction, resulting from the rapid decrease in density with increasing height in the Jovian atmosphere, causes an apparent defocusing of light passing through the atmosphere from the solar source to an observer situated on the illuminated disk of the satellite. With reference to Figure 3.2, the radiation flux per cm^2 from the point source S, at a distance l from the limb of the planet, has been attenuated by the factor F because of differential refraction in the atmosphere. The factor F is given by

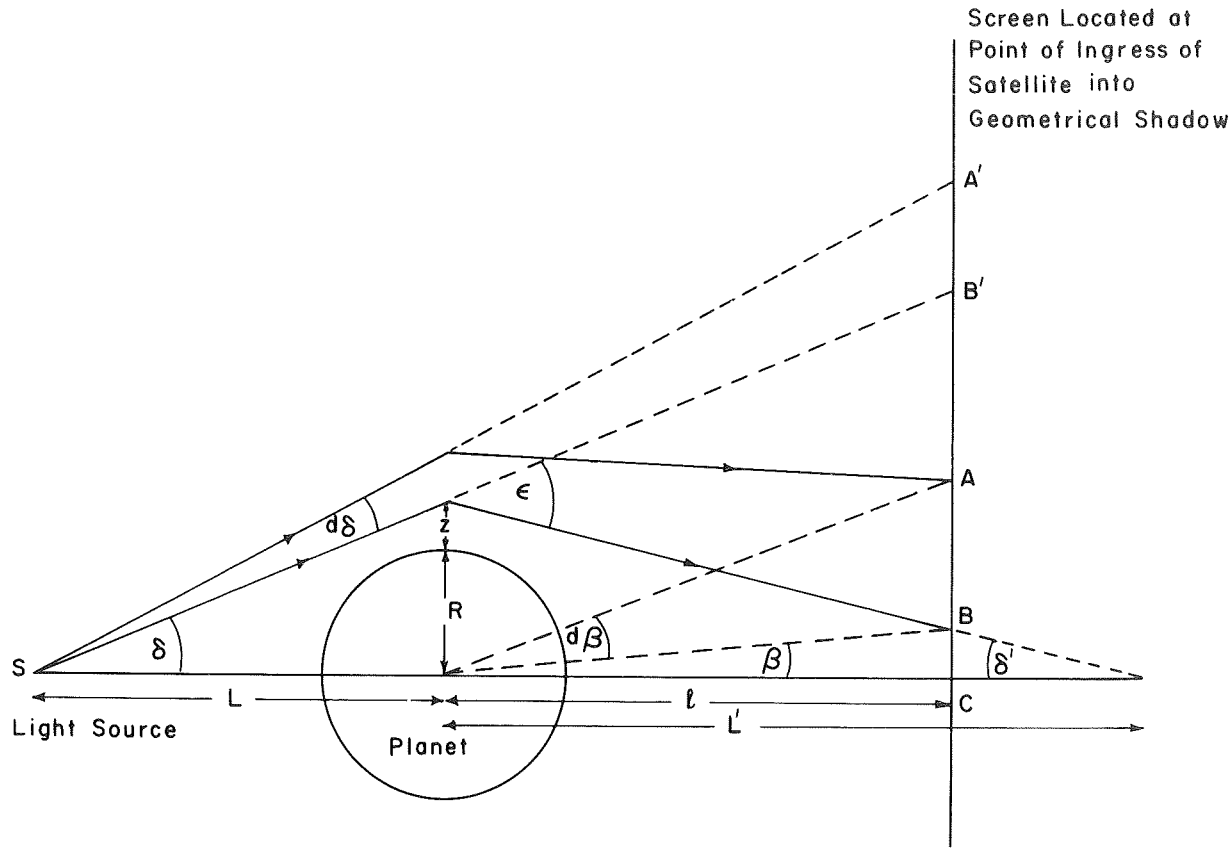

Figure 3.2—Schematic representation of the geometry of differential refraction in a planetary atmosphere. Point light source assumed.

$$F = \frac{ds'}{ds}, \tag{3.80}$$

where ds is the area of the ring surface that would be produced by the unrefracted light beam in the distance l if the planet did not possess an atmosphere. The quantity ds' is the corresponding area of the ring surface which is produced by the refracted light beam in the same distance. By elementary considerations ds is given by

$$ds = 2\pi\,(L + l)\,\delta\,(L + l)\,d\delta \tag{3.81}$$

and ds' is given by

$$ds' = 2\pi\, l\, \beta\, l\, d\beta\,, \tag{3.82}$$

so that

$$F = \frac{ds'}{ds} = \frac{2\pi l^2 \beta\, d\beta}{2\pi(L + l)^2\, \delta d\delta} = \frac{l^2 \beta\, d\beta}{(L + l)^2\, \delta d\delta}. \tag{3.83}$$

For Equation 3.83 to be valid, both δ and β must be small, which is the case of interest to us.

From Figure 3.2,

$$\delta = \frac{R + z}{L} . \tag{3.84}$$

where R is the radius of the planet and z is the height above the surface at closest approach of the narrow beam of light to the center of the planet. In addition,

$$\delta' = \frac{R + z}{L'} = \epsilon - \delta , \tag{3.85}$$

where ϵ is the angle through which the beam of light is refracted. From Equations 3.84 and 3.85 it follows that

$$\beta = \frac{BC}{l} = \frac{(L' - l)}{l} \delta' = \frac{L' \delta'}{l} - \delta' \tag{3.86}$$

or

$$\beta = \frac{(R + z)}{l} - \epsilon + \delta . \tag{3.87}$$

Using Equation 3.84 we obtain

$$\beta = \frac{(R + z)}{l} + \frac{(R + z)}{L} - \epsilon . \tag{3.88}$$

By differentiating Equation 3.88 with respect to z, we obtain

$$\frac{d\beta}{dz} = \frac{1}{l} + \frac{1}{L} - \frac{d\epsilon}{dz} = \frac{(L + l)}{lL} - \frac{d\epsilon}{dz} . \tag{3.89}$$

By differentiating Equation 3.84 with respect to z, we obtain

$$\frac{d\delta}{dz} = \frac{1}{L} . \tag{3.90}$$

By replacing the derivatives in Equations 3.89 and 3.90 by finite differences, we may substitute for $d\beta$ and $d\delta$ in Equation 3.83 and obtain

$$F = \frac{l^2 \left[\frac{(R + z)}{lL} (l + L) - \epsilon\right] - \left[\frac{(L + l)}{lL} - \frac{d\epsilon}{dz}\right]}{(L + l)^2 \frac{(R + z)}{L} \frac{1}{L}} . \tag{3.91}$$

After some simple algebraic manipulations, we obtain

$$F = \left[1 - \frac{\epsilon L\, l}{(R+z)(L+l)}\right]\left[1 - \frac{d\epsilon}{dz}\frac{lL}{(L+l)}\right]. \tag{3.92}$$

If, for simplicity, we write

$$\lambda_1 = \frac{lL}{(l+L)}, \tag{3.93}$$

then Equation 3.92 becomes

$$F = \left[1 - \frac{\lambda_1 \epsilon}{(R+z)}\right]\left[1 - \lambda_1 \frac{d\epsilon}{dz}\right]. \tag{3.94}$$

By differentiating Equation 3.60 with respect to height, we can readily show that

$$\frac{d\epsilon}{dz} = -\frac{\epsilon}{H}. \tag{3.95}$$

Equation 3.94 may, therefore, be rewritten as

$$F = \left[1 - \frac{\lambda_1 \epsilon}{(R+z)}\right]\left[1 + \frac{\lambda_1 \epsilon}{H}\right]. \tag{3.96}$$

Equation 3.96 requires $\lambda_1 \epsilon \leq (R + z)$ if F is to be always both positive and finite; i.e., the displacement of the beam on the fictitious screen must be less than the radius of the planet. Since in the cases of interest to us $\lambda_1 \epsilon << R$, Equation 3.96 may be used without difficulty.

In the case where the point source S is replaced by the Sun, the planet is Jupiter, and the screen is replaced by one of the Galilean satellites entering eclipse, Equation 3.96 may be rewritten as

$$F = \left[1 - \frac{\lambda_1 \epsilon}{(r_0 + h_0)}\right]\left[1 + \frac{\lambda_1 \epsilon}{H}\right] \tag{3.97}$$

or to a good approximation

$$F = \left(1 - \frac{\lambda_1 \epsilon}{r_0}\right)\left(1 + \frac{\lambda_1 \epsilon}{H}\right). \tag{3.98}$$

The quantity λ_1 is then given by

$$\lambda_1 = \frac{d_0\, d_1}{d_0 + d_1}, \tag{3.99}$$

where d_1 is the distance of Jupiter from the Sun. To a good approximation

$$\lambda_1 = d_0 , \tag{3.100}$$

since $d_1 >> d_0$.

H. Resolution of the Jovian Atmosphere

The physical structure of the Jovian atmosphere may be well resolved in both latitude and longitude by studying the refraction tails of the ingress light curves of the Galilean satellites. For the simplified geometrical situation considered in this paper, each of the satellites will enter the Jovian shadow in a direction normal to its edge. Resolution of the atmosphere in latitude will be good because the diameter of each of the satellites is only a small fraction of the diameter of the planet. The angular resolution of the circumference of the Jovian disk will be equal to the ratio of the diameter of the satellite to the radius of the planet. In the case of the mean satellite entering eclipse, the resolution in latitude will, therefore, be equal to 3.2°. In addition, for the simplified geometrical situation only, the refraction tail of the light curve will span zero range in latitude. Resolution of the atmosphere in longitude will also be good because most of the refraction and scattering suffered by a ray of light traversing the atmosphere will occur near the point of closest approach to the center of the planet. From Equations 3.60 and 3.79, it is clear that most of the interaction of radiation with the atmosphere will occur within a path length of $(2\pi RH)^{1/2}$ centered on the point of closest approach of the ray to the center of the planet. The resolution of the atmosphere in longitude will, therefore, be approximately equal to $(2\pi H/R)^{1/2}$ radians. Numerically, the resolution in longitude will be about 1.6 degrees, if H is 8.3 km. If the geometrical situation is more complex, with the satellite entering eclipse in a direction other than normal to the edge of the Jovian shadow, the refraction tail of the light curve will span a finite range in latitude, and the resolution in longitude will deteriorate.

The geometry related to the resolution in height of the Jovian atmosphere at any particular point on the refraction tail of one of the ingress light curves is shown in Figure 3.3. For simplicity we will consider only the period during ingress when every point on the disk of the satellite is illuminated by refracted rays of light from every part of the solar disk. The entire refracted solar disk, albeit distorted, is visible to an observer located at any point on the illuminated hemisphere of the satellite. Ingress has not yet progressed to the point where the refracted solar disk would appear to be truncated, because the limiting angle of refraction ϵ_{limit}, for rays of light grazing either the cloud tops or the level of critical refraction, has not yet been reached for any point on the disk of the satellite.

Consider first the case where the level of critical refraction is below the cloud tops. A ray of light traversing the atmosphere will be refracted through the maximum possible angle ϵ_0, when its point of closest approach to the center of the planet is an infinitesimal distance above the clouds. In this case we have

$$\epsilon_{\text{limit}} = \epsilon_0 . \tag{3.101}$$

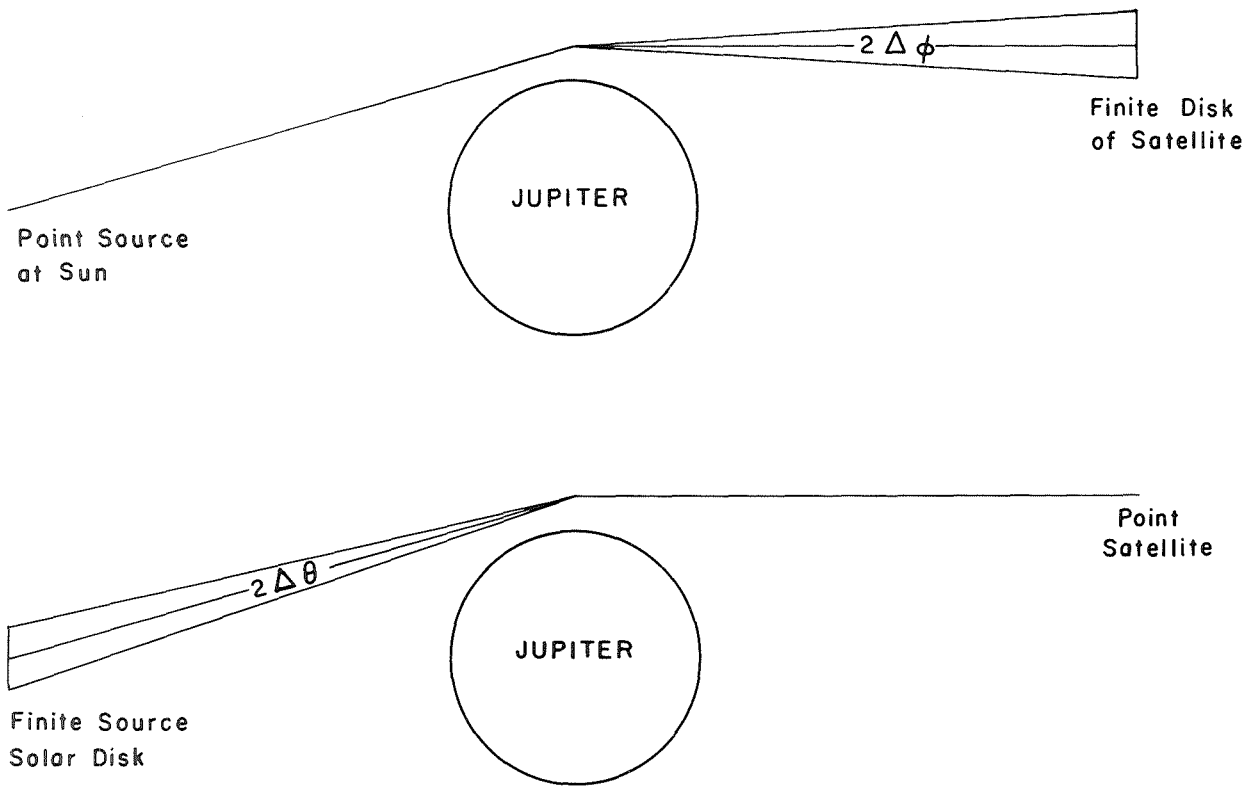

Figure 3.3—Schematic geometry to demonstrate height resolution of the atmosphere at any point on the refraction tail of the ingress light curve. The effects of the finite sizes of both the solar source and the satellite on the spread in the angle of refraction are shown.

Consider next the case where the level of critical refraction is above the cloud tops. Here, a ray of light traversing the atmosphere will be refracted through the maximum possible angle $\epsilon_{\text{critical}}$, when its point of closest approach to the center of the planet is an infinitesimal distance above the level of critical refraction. In this case we have

$$\epsilon_{\text{limit}} = \epsilon_{\text{critical}} . \tag{3.102}$$

For any chosen model atmosphere, it is a simple matter to determine at what level critical refraction occurs for light of any particular wavelength, and to determine whether that level is above or below the cloud tops.

The height h_c of closest approach to the cloud tops for the ray of light joining the centers of the disks of the Sun and the satellite may be obtained from

$$\epsilon_c = \epsilon_0 \exp\left(-\frac{h_c}{H}\right), \tag{3.103}$$

where ϵ_c is the angle of refraction which is required. For the ray to pass through the atmosphere, ϵ_c must be less than both ϵ_0 and $\epsilon_{\text{critical}}$.

By differentiating Equation 3.61 with respect to h_0, we may obtain a relation between $\Delta\Phi$, the angular radius of the satellite viewed from the limb of Jupiter; $\Delta\theta$, the angular radius of the Sun viewed from the limb of Jupiter; and Δh_0, the spread in height of the light rays, which illuminate the disk of the satellite, at their closest approach to the center of the planet. We have

$$\frac{d\epsilon}{dh_0} = -\frac{\epsilon}{H}, \tag{3.104}$$

which may be written in finite form as

$$\Delta h_0 = H\frac{|\Delta\epsilon|}{\epsilon_c}, \tag{3.105}$$

where $2\Delta\epsilon$, the required spread in the angle of refraction, follows from

$$\Delta\epsilon = \Delta\Phi + \Delta\theta . \tag{3.106}$$

The height resolution is, therefore, $2\Delta h_0$.

Since $\Delta\theta$ is finite, the beginning of the refraction tail to the ingress light curve occurs when the center of the disk of the satellite is more than one satellite radius within the reference edge of the Jovian shadow. For that particular geometry we have

$$\epsilon_c \cong \Delta\Phi , \tag{3.107}$$

since reference to Tables 2.1, 2.2, and 2.3 shows that

$$\Delta\theta << \Delta\Phi . \tag{3.108}$$

It follows, in this case, that

$$\Delta h_0 \cong H , \tag{3.109}$$

and the height resolution, therefore, is $2H$.

As ingress of the satellite into eclipse progresses further, the required value of ϵ_c rapidly increases and the height resolution improves according to Equation 3.105. The resolution continues to improve as ϵ_c approaches ϵ_{limit}, and h_c gradually decreases. Specifically, a height resolution of one scale height is obtained quite close to the beginning of the refraction tail when

$$\epsilon_c \cong 2\Delta\Phi . \tag{3.110}$$

Two special regions of the ingress light curve have not been considered here because it is very difficult to make use of them in resolving the structure of the Jovian

atmosphere. The first region occurs at the very beginning of ingress when part of the disk of the satellite is illuminated by direct sunlight and the other part is illuminated by sunlight refracted through the Jovian atmosphere. Here the part of the disk directly illuminated dominates in determining the character of the light curve. It is extremely difficult, therefore, to extract any information about the refraction properties of the Jovian atmosphere from this portion of the light curve. The situation does not improve until the area of the disk that is directly illuminated approaches zero. The second region occurs at the end of ingress when the disk of the satellite is no longer fully illuminated by refracted solar radiation and is almost totally eclipsed. Some regions of the disk are still receiving radiation from a refracted solar disk, which now appears to be increasingly truncated. Other regions no longer receive any refracted solar radiation at all because the limiting angle of refraction ϵ_{limit} has been reached for all regions of the solar disk. At this point during ingress, variations of the reflectivity over the disk of the satellite may arbitrarily and appreciably alter the character of the light curve as the illuminated area of the disk becomes smaller and smaller. In addition, accurate photometry of this region of the light curve would be extremely difficult since the light levels are very low.

Compared with the effects of the finite sizes of the Sun and the satellite, diffraction is of negligible importance in limiting the height resolution of the atmosphere attainable by the eclipse technique. If we assume that Jupiter possesses no atmosphere, but has a very sharply defined limb, and that the mean satellite is reduced to a point, we can apply Fresnel's theory for the case of diffraction by a straight edge to determine the limit to height resolution imposed by diffraction. For radiation of wavelength 5500Å, the diffraction limit is of the order of 15 m. However, since the diffraction limit varies as $\lambda^{1/2}$, diffraction severely limits the effectiveness of any spacecraft flyby radio beam occultation experiment to resolve the physical structure of the Jovian atmosphere. Such occultation experiments normally utilize radiation transmitted in the S-band (1000 to 5000 MHz). Consequently, the height resolution attainable using spacecraft flybys of the planet will be no better than 5 to 11 km, i.e., of the same order as the scale height.

I. Effects of Solar Disk Limb Darkening and Finite Size of Satellite

As viewed from any one of the Galilean satellites, the angular diameter of the Sun is very much smaller than the angular diameter of the Jovian disk. Consequently, the curvature of the Jovian atmospheric strata can be neglected in determining the flux of radiation incident on the disk of the satellite at any instant during ingress. Also, because the linear diameter of the satellite is very much smaller than the linear diameter of the Jovian shadow, we can neglect the apparent curvature of its reference edge projected onto the disk of the satellite.

To determine the illumination of any selected point on the disk of the satellite, the apparent disk of the Sun is divided into linear strips of equal angular width parallel to the limb of Jupiter and perpendicular to the shortest line from the center of the solar disk to the reference edge of the Jovian shadow. Each solar strip must be considered individually to determine its contribution to the illumination of the chosen point. First, it must be decided whether the particular selected strip is visible to an observer situated

at the chosen point. To obtain this information, the required value of ϵ must be determined by simple geometrical considerations. If $\epsilon \leq 0$, it will not be necessary for light from the solar strip to pass through the Jovian atmosphere and be refracted in order to reach the observer. The observer, therefore, receives direct and unattenuated radiation from the solar strip. If $\epsilon > 0$, it will be necessary for the light to pass through the atmosphere and suffer refraction and attenuation in the process. In particular, if $\epsilon > \epsilon_{limit}$, the solar strip will be completely invisible to the observer. For the case where $0 < \epsilon \leq \epsilon_{limit}$, the theory described earlier may be used to calculate the total extinction suffered by the light on its way to the observer. Summation of the contributions from all strips enables the illumination of the observer to be determined.

In the foregoing discussion it is implied that each solar strip is of equal area and brightness. In fact, of course, this is not so, and due consideration must be given to the circular shape of the solar disk and also to its limb darkening. Each strip must be weighted accordingly. Figure 3.4 shows the Sun and the geometry associated with the limb-darkening problem.

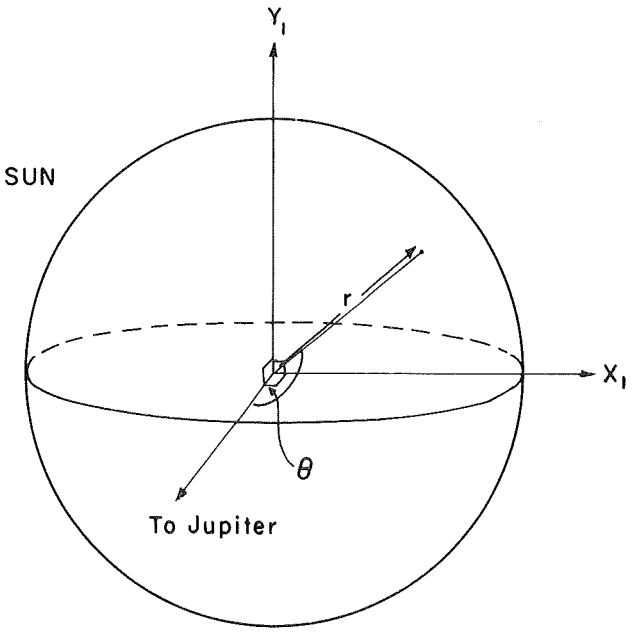

Figure 3.4—The Sun and the geometry associated with the limb-darkening problem.

To a good approximation the solar limb darkening is given by

$$I_\lambda(\theta) = I_\lambda(0)\,(1 - u_1 + u_1 \cos\theta)\,, \quad (3.111)$$

where $I_\lambda(\theta)$ is the intensity of radiation of wavelength λ at position θ on the solar disk (the angle θ is defined in Figure 3.4). The parameter labeled here as u_1 is the limb-darkening coefficient, tabulated as a function of λ by Allen (1963). We may write

$$\sin\theta = \frac{\sqrt{X_1^2 + Y_1^2}}{r} \quad (3.112)$$

and

$$\cos\theta = \sqrt{1 - \left(\frac{X_1^2 + Y_1^2}{r^2}\right)}\,, \quad (3.113)$$

where r denotes here the solar radius. By transformation, we obtain

$$X = \frac{X_1}{r} \quad \text{and} \quad Y = \frac{Y_1}{r}\,, \quad (3.114)$$

where all units of length are normalized to the solar radius as unity. Equation 3.111 may now be rewritten as

$$I_\lambda(\theta) = Q\left[1 + \beta'\sqrt{1 - (X^2 + Y^2)}\right], \quad (3.115)$$

where

$$Q = I_\lambda(0)(1 - u_1) \tag{3.116}$$

and

$$\beta' = \frac{u_1}{(1 - u_1)} . \tag{3.117}$$

We can define the quantity $A(X)\,dX$ to be the fraction of solar radiation in a linear strip across the solar disk between X and $X + dX$. We normalize $A(X)\,dX$ so that the total brightness of the apparent solar disk is unity. In that case we have

$$\int_{-1}^{+1} A(X)dX = 1 . \tag{3.118}$$

We can then write

$$A(X) = \frac{\displaystyle\int_{Y=0}^{\sqrt{1-X^2}} \left[1 + \beta' \sqrt{1 - (X^2 + Y^2)}\right] dY}{\displaystyle\int_{X=-1}^{+1} \int_{Y=0}^{\sqrt{1-X^2}} \left[1 + \beta' \sqrt{1 - (X^2 + Y^2)}\right] dY\, dX} . \tag{3.119}$$

The evaluation of these integrals is straightforward, and their solution gives

$$A(X) = \frac{\frac{2}{\pi}\sqrt{1 - X^2} + \frac{\beta'}{2}(1 - X^2)}{\left(1 + \frac{2}{3}\beta'\right)} . \tag{3.120}$$

To determine the total brightness of the satellite during ingress, its disk is divided into linear strips of equal width perpendicular to the shortest line from the center of the satellite to the reference edge of the Jovian shadow. The illumination of a typical point within each strip may then be determined as outlined above. If the disk of the satellite is uniformly reflective, the contribution of each strip to the total brightness of the satellite is determined by its area. With reference to Figure 3.5, the disk of the satellite is assumed to be of unit radius and to be divided into n linear strips of equal width. The area B_i of a particular strip i is given by

$$B_i = 2\sqrt{1 - X_i^2}\ \Delta X , \tag{3.121}$$

where the width ΔX is $2/n$, and X_i may take any of the values 0, $\pm 2/n$, $\pm 4/n$, etc. Because the total area of the stips will closely approximate the area of the disk, it follows that

$$\sum_{i=1}^{n} B_i = \pi \tag{3.122}$$

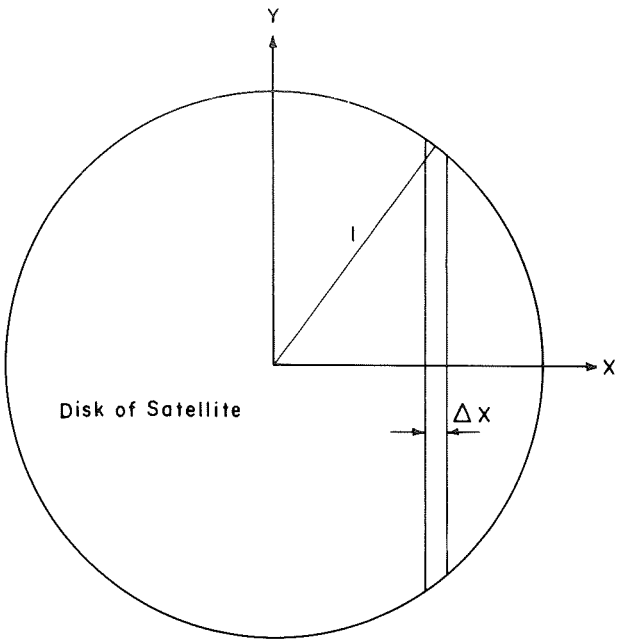

Figure 3.5—The disk of the satellite divided into strips of equal width ΔX.

if we normalize the area of the disk to unity. It follows that

$$B_i = \frac{2}{\pi}\sqrt{1 - X_i^2}\ \Delta X . \qquad (3.123)$$

Summation of all contributions permits the total brightness of the satellite to be determined at the particular chosen instant during ingress.

The assumption that the disk of the satellite is perfectly circular is an excellent one. Even when Jupiter is at quadrature, the defect of illumination is quite negligible. The assumption that the disk is uniformly reflective is, however, questionable. The effect on the ingress light curve of an arbitrary distribution of reflectivity over the surface of the satellite will be discussed later.

For convenience in carrying out the numerical integrations, both the apparent solar disk and the disk of the satellite are divided into 50 linear strips of equal width. Numerical experiments, with 200 strips each, showed a negligible improvement in accuracy in the determination of the ingress light curve.

Further experiments showed that if less than 20 strips each are used, the accuracy of the calculation is decreased.

CHAPTER 4

APPLICATION OF THE THEORY TO THE INFERENCE OF THE PHYSICAL PROPERTIES OF THE JOVIAN ATMOSPHERE

A. Ingress Light Curve at Visual Wavelengths: Mean Satellite and Standard Model of Jovian Atmosphere

The ingress light curve for the mean satellite and the standard model of the Jovian atmosphere is shown in Figure 4.1. The wavelength selected for the calculation of the light curve was 5500Å. In the region of the curve $-250 \text{ sec} < t < 250 \text{ sec}$, the brightness of the satellite is determined largely by the contribution from the directly illuminated part of its disk. The refraction tail of the light curve does not begin until t is approximately 250 sec. For the region of the curve with t greater than 250 sec, the satellite is completely within the Jovian shadow. No part of the disk of the satellite can then receive solar radiation directly. However, for some considerable time, the satellite continues to be illuminated by an envelope of light rays from the Sun that have been refracted through the Jovian atmosphere. As t continues to increase, the brightness of the satellite steadily decreases. As t advances, each of the light rays in the envelope must penetrate increasingly deeper into the atmosphere in order to suffer sufficient refraction to reach the disk of the satellite. Deeper penetration produces increased attenuation. Eventually the limiting angle of refraction is reached. Thereafter, as t continues to

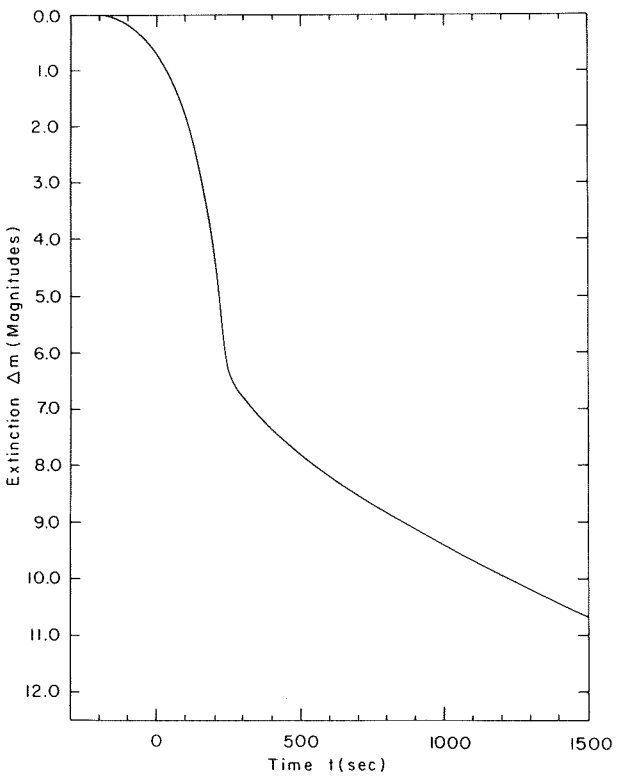

Figure 4.1—The ingress light curve for the mean satellite. Standard model of Jovian atmosphere: λ 5500Å.

increase, the light curve rapidly becomes truncated. The location in time of the cutoff region in the light curve is directly related to the limiting angle of refraction in the atmosphere. It will be shown later that, for the adopted standard model atmosphere, ϵ_{limit} is reached for $t > 1500$ sec. Consequently, the cutoff in the light curve does not appear in Figure 4.1. Beyond the cutoff region, the satellite is illuminated only by diffuse solar radiation which has been multiply scattered in the Jovian atmosphere. It will be shown later that this source of illumination contributes very little to the brightness of the satellite.

The degree of sharpness associated with the edge of the Jovian shadow, for the case of the standard atmosphere and a wavelength of 5500Å, is indicated by the two curves in Figure 4.2. Curve I refers to the case of a point satellite, with the Sun reduced to a point source. For the purpose of the calculation, the radius of the satellite was set equal to 1 cm, with the angular radius of the Sun set equal to 0".01. Curve II refers to the case of a point satellite (i.e., radius 1 cm) but with a finite Sun whose angular radius is that appropriate for an observer at the distance of Jupiter from the Sun (i.e., 184".45).

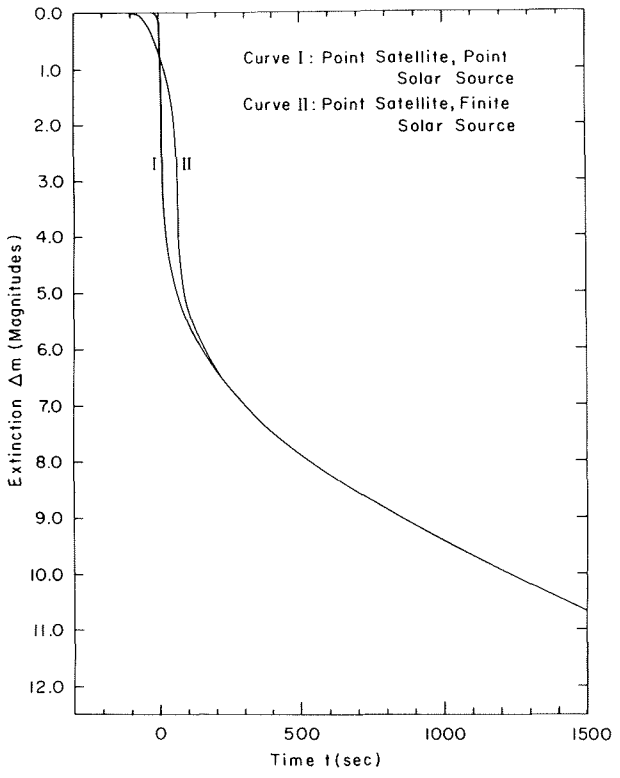

Figure 4.2—The degree of sharpness associated with the edge of the Jovian shadow. Curve I: Point solar source, point satellite. Curve II: Finite solar source, point satellite. Standard atmosphere: λ 5500Å.

B. Effect of Variation in the Scale Height of the Atmosphere

The effect of variation in the scale height of the Jovian atmosphere on the ingress light curve for the mean satellite, at a wavelength of 5500Å, is shown in Figure 4.3. The standard values for both the H_2/He ratio and the pressure at the cloud tops were used in the calculation. Because the atmosphere is assumed to be isothermal and homogeneous, the scale height H is independent of height above the clouds. The temperature T, associated with the chosen scale height, may be obtained from

$$H = \frac{RT}{\mu g} \qquad (4.1)$$

where, here, R is the gas constant, g is the surface gravity for Jupiter, and μ is the mean molecular weight appropriate for the chosen H_2/He ratio. The standard value for the atmospheric temperature enters into the calculation of each light curve, but only to determine the number density N_0 at the cloud tops from the perfect gas law.

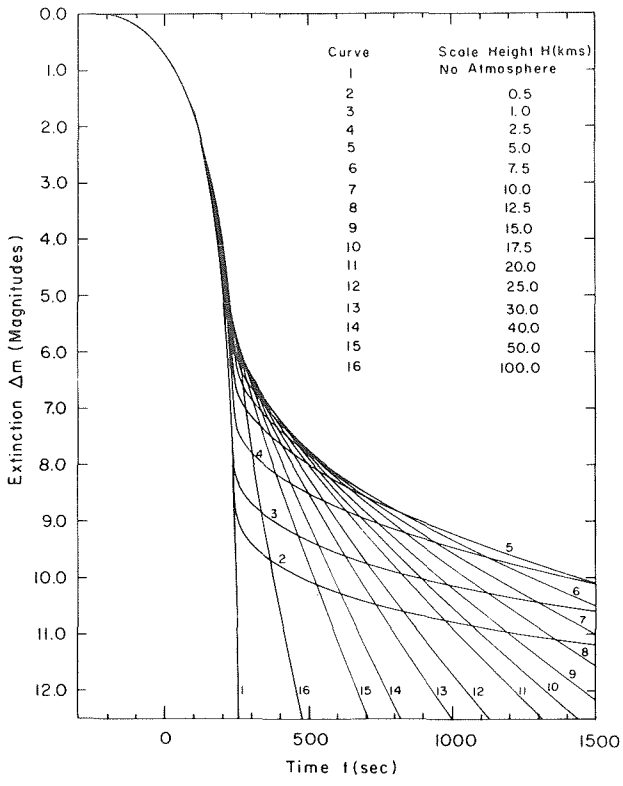

Figure 4.3—The effect of variation in the scale height of the Jovian atmosphere on the ingress light curve for the mean satellite. Standard atmosphere assumed except for variation of scale height: λ 5500Å.

The light curve that would result if Jupiter had no atmosphere is plotted in Figure 4.3 as Curve 1. The other curves, numbered 2 through 16, show the refraction tails produced by various model atmospheres for a range of scale heights between 0 and 100 km. If the standard value for the scale height is adopted, the corresponding light curve will lie between curves 6 and 7. It is clear that the ingress light curve is insensitive to the effects of atmospheric refraction for extinctions of less than 5 or 6 magnitudes. In fact, to be able to differentiate clearly between one model atmosphere and another, it is necessary to study the light curve for much greater extinctions. It is clear from Figure 4.3 that if accurate observations of the light curve could be made for extinctions up to and beyond 10 magnitudes, the scale height could be very accurately determined, provided the H_2/He ratio by numbers was known. Just how such observations can be made will be thoroughly discussed later. If, however, it is assumed that the refraction tail can be located at 10 magnitudes extinction with an uncertainty of ± 0.1 magnitudes, then the accuracy to be expected in the determination of the scale height can be estimated. If the true curve lies between curves 6 and 7, the scale height can be determined to an accuracy of ± 1 km if the H_2/He ratio is known exactly. A precise knowledge of the H_2/He ratio is not strictly necessary, however, because the refraction tail is relatively insensitive to the helium content of the atmosphere. In fact, as will be shown later, if the H_2/He ratio is near the standard value of 5.1, an uncertainty in the helium content of ± 100 percent will produce an uncertainty in the derived scale height of approximately ± 1 km only. In that case, the limiting accuracy attainable in the determination of the scale height would be ± 2 km.

It may be noted that the scale height computed from the standard values for the temperature and H_2/He ratio is inconsistent with the value obtained by Baum and Code (1953). If it is assumed that the atmosphere is composed of a mixture of H_2 and He only, with the adopted H_2/He ratio of 5.1, the mean molecular weight is 2.33. The corresponding scale height for a temperature of 145°K is approximately 21 km, which is substantially different from the value of 8.3 km (± 50 percent) obtained by Baum and Code. Clearly, the precise value for the scale height is very uncertain at the present time. Further observations of stellar occultations and of eclipses of the Galilean satellites, together with

radio wave occultation experiments performed using flyby spacecraft, are required to improve our knowledge of the Jovian scale height.

C. Height Resolution of the Atmosphere

In Figure 4.4 the ingress light curve of the mean satellite at a wavelength of 5500Å, for the case of the standard Jovian atmosphere, is reproduced from Figure 4.1. Also shown is the corresponding curve of height resolution of the atmosphere as a function of time. The curve of height resolution as a function of time begins at the instant during ingress when no part of the disk of the satellite is illuminated by direct sunlight. As ingress continues beyond this point, the height resolution rapidly improves. From a value of $2H$—twice the scale height — at the beginning of the refraction tail, it improves to approximately 0.5 H at an extinction near 10 magnitudes. Reference to the theoretical section on resolution of the atmosphere shows that the curve of height resolution as a function of time is independent of wavelength.

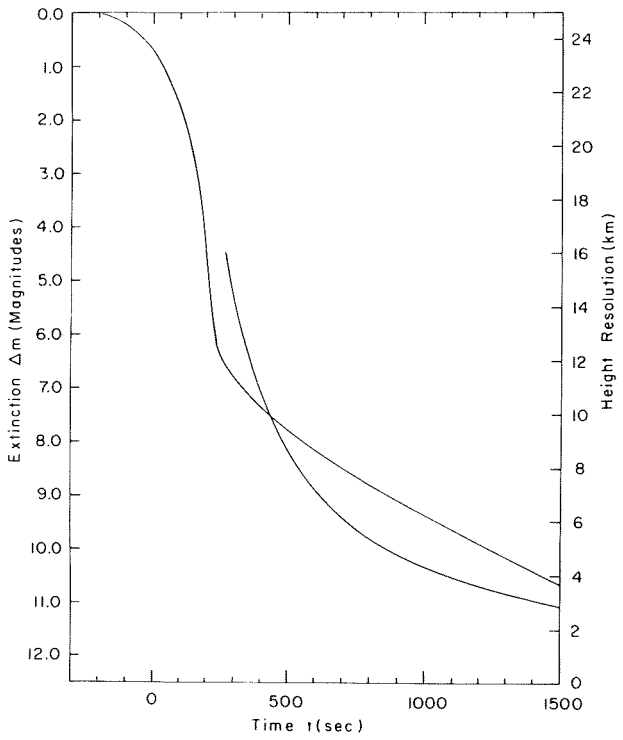

Figure 4.4—Height resolution as a function of time during ingress of the mean satellite. Standard atmosphere assumed. Ingress light curve of Figure 4.1 also plotted.

Figure 4.5 shows the ingress light curve reproduced from Figure 4.1 together with the curve of h_c as a function of time. As before, the quantity h_c is the height above the clouds of closest approach to the center of the planet for a refracted ray of light connecting the center of the solar disk with the center of the disk of the satellite. The curve of h_c as a function of time begins at the same instant as the curve of height resolution as a function of time. Figure 4.5 shows that the standard atmosphere can be scanned in height from approximately 37.5 km above the clouds downward by studying the refraction tail for radiation of a wavelength of 5500Å. At an extinction of 10 magnitudes, h_c is close to 25 km. The value of h_c continues to decrease as time increases. The curve of h_c as a function of time is weakly dependent on wavelength since ϵ is a weak function of wavelength.

Figure 4.6 shows the ingress light curve of Figure 4.1 again, but this time plotted with the curve of $N(h_c)$ as a function of time. The quantity $N(h_c)$ is the number density corresponding to the height h_c above the clouds. The curve of $N(h_c)$ as a function of time is also weakly dependent on wavelength.

The refraction tail shown in Figure 4.1 contains information concerning a much lower region of the Jovian atmosphere than does the light curve for a stellar occultation.

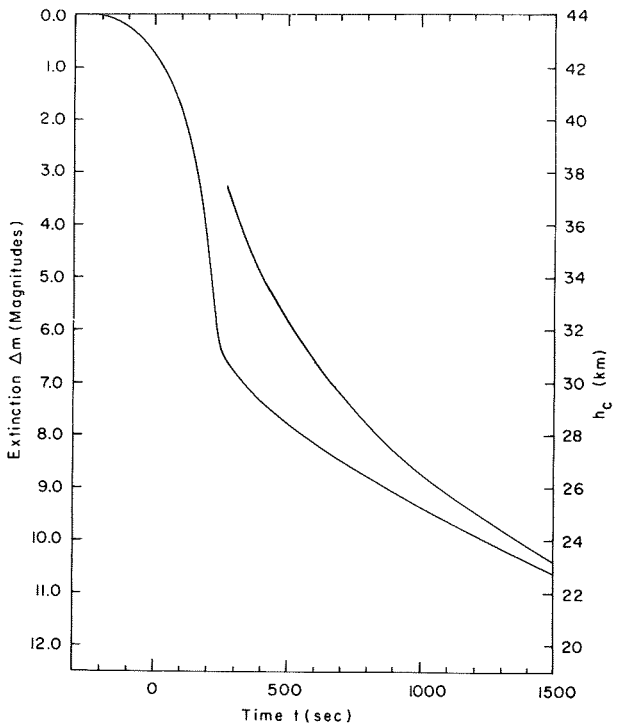

Figure 4.5—Height h_c of closest approach above the clouds of a light ray, connecting the center of the solar disk with the center of the disk of the mean satellite, from the center of Jupiter as a function of time. Standard atmosphere assumed. Ingress light curve of Figure 4.1 also plotted.

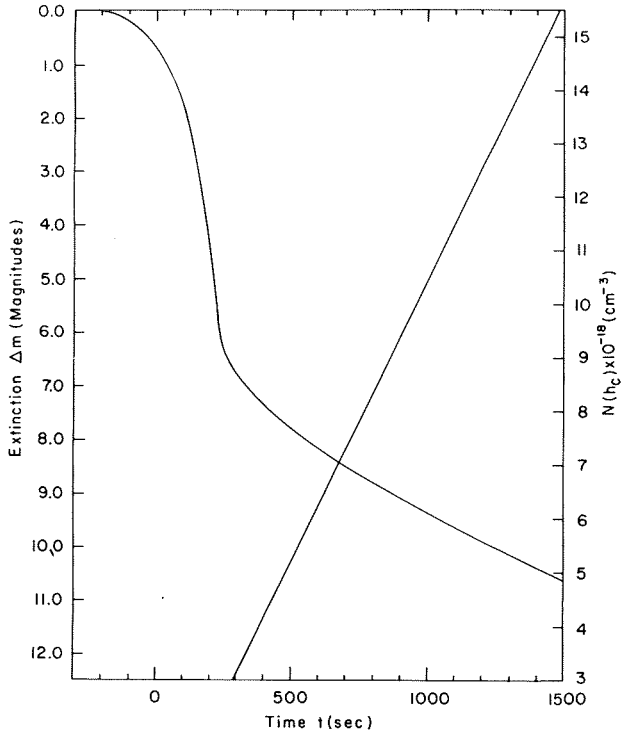

Figure. 4.6—Number density $N(h_c)$ corresponding to height h_c as a function of time. Standard atmosphere assumed. Ingress light curve of Figure 4.1 also plotted.

This refraction tail contains information on the properties of the atmosphere below h_c = 37.5 km, corresponding to number densities above 2.83×10^{18} cm^{-3}. In the case of a stellar occultation observed from Earth, the number density and height, corresponding to the half-intensity point on the light curve, can be readily calculated by the method used by Hunten and McElroy (1968) in their analysis of observations of an occultation of Regulus by Venus. The half-intensity point on the light curve observed by Baum and Code (1953) for the occultation of σ Arietis by Jupiter corresponds to a number density in the standard Jovian atmosphere of 1.32×10^{13} cm^{-3} and to a corresponding height of 139.3 km. Examination of the light curve obtained by Baum and Code shows that the brightness of the star dropped from nearly 100 percent to near zero percent in approximately 10 sec. Because the apparent velocity of the star normal to the limb of the planet at the point of ingress was 12.0 km/sec, the observed light curve corresponds to a range in height of approximately ±60 km centered on a height of 139.3 km.

D. Effect of Variation in the H_2/He Ratio for the Atmosphere

Figure 4.7 shows the effect of variations in the H_2/He ratio on the ingress light curve for the mean satellite at a wavelength of 5500Å. Throughout the calculation, the other atmospheric parameters were fixed at their standard values. Curves 1 through 6

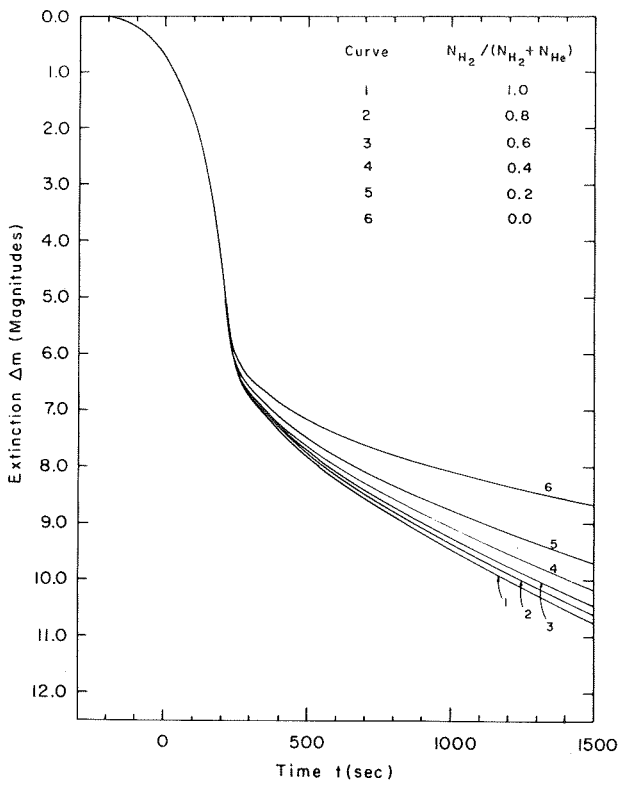

Figure 4.7--The effect of variation in the H_2/He ratio in the Jovian atmosphere on the ingress light curve for the mean satellite. Standard atmosphere assumed apart from variation in the H_2/He ratio: λ 5500Å.

show the effect of varying the parameter $N_{H_2}/(N_{H_2} + N_{He})$ from 0 to 1 in steps of 0.2. As before, the quantities N_{H_2} and N_{He} refer to the number densities of H_2 and He respectively. Because the atmosphere is assumed to be homogeneous, the parameter $N_{H_2}/(N_{H_2} + N_{He})$ is invariant with the height above the clouds.

Figure 4.7 shows that the refraction tail of the light curve is insensitive to the precise value for the H_2/He ratio, if the helium content of the Jovian atmosphere is small. The insensitivity results from the relative inefficiency of helium to refract and scatter radiation. If the H_2/He ratio is greater than unity it is extremely difficult to infer the helium content of the atmosphere, even if the scale height is known accurately as a function of height. Consider, for example, the case where the Jovian atmosphere is well represented by the standard model. If observations of the light curve were made down to an extinction of 10 magnitudes, with an accuracy of ±0.1 magnitudes, the helium abundance derived from the shape of the refraction tail would be uncertain by at least ±100 percent

E. Effect of Variation in the Wavelength

Figure 4.8 shows the effect of varying the wavelength on the ingress light curve for the mean satellite. The standard model of the Jovian atmosphere was used in the calculation. Curves 1 through 5 are the light curves for a range in wavelength from 4000Å to 8000Å. Each curve has been normalized to eliminate any effect caused by variation of the surface reflectivity of the satellite with wavelength. Figure 4.8 shows clearly that the refraction tail is sensitive to variation in the wavelength. The prime reason for the sensitivity is the pronounced variation with wavelength of the effective Rayleigh scattering cross section. At any selected time on the refraction tail of the light curve, the normalized brightness of the satellite is a function of wavelength. The functional dependence is determined by the optical scattering properties of the chosen model of the Jovian atmosphere.

The degree of sharpness of the cloud tops, as a function of wavelength, is of considerable interest at the present time. Owen and Mason (1968) have discussed the growing body of photometric and spectroscopic evidence that indicates that the cloud tops are rather hazily defined. In particular, the height of the effective level of reflection appears

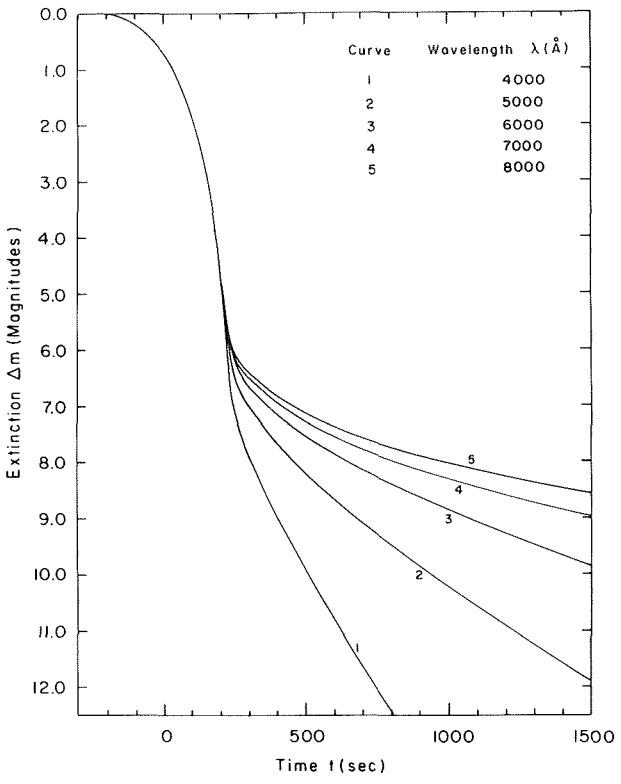

Figure 4.8—The effect of variation in the wavelength on the ingress light curve for the mean satellite. Standard Jovian atmosphere assumed. Wavelengths between λ 4000Å and λ 8000Å considered.

to be a function of both wavelength and latitude. At higher latitudes the cloud level appears to be somewhat lower than at latitudes near the equator. In addition, the height of the effective level of reflection appears to increase with decreasing wavelength. Multicolor photometry of the refraction tail will permit the optical scattering properties of the interface between clear and cloudy regions of the Jovian atmosphere to be well studied. The observations may be compared readily with theoretical predictions for a clear Rayleigh scattering atmosphere above a thick cloud layer. Disagreement between theory and observation is to be expected if additional scattering, produced by a haze of cloud particles, occurs in this supposedly clear region of the atmosphere. The optical scattering properties of the cloud particles may be inferred and limits placed on their probable size and number density as functions of height. Such information will prove useful in checking theories of the nature of the clouds in the Jovian atmosphere.

How high the haze extends above the thick cloud level is not known. It is interesting to speculate that if it should extend to a height corresponding to a number density of order 10^{13} cm^{-3} it might severely distort the light curve for a stellar occultation observed from Earth. During such occultations, differential refraction in the supposedly clear regions of the atmosphere high above the cloud layer produces the observed light curve. Rayleigh scattering at such levels is minimal. If there should be a significant haze of cloud particles in that part of the atmosphere, attenuation by scattering would result. Since we would expect the number density of cloud particles in the haze to increase with decreasing height, the net effect would be to steepen the occultation light curve. Unless the effects of such a haze were taken into account in the analysis of the light curve, the scale height would be underestimated. Haze may, therefore, account for the apparent inconsistency between the value of the scale height obtained by Baum and Code (1953) and the value obtained by calculation from the standard values of temperature and H_2/He ratio for the Jovian atmosphere.

F. Effect of Uncertainty in the Radii of the Satellites

The precise shape of the ingress light curve for each of the Galilean satellites depends on the value adopted for its radius. How reliably the physical properties of the

Jovian atmosphere may be inferred from the refraction tails of the light curves is related to how accurately the radii of the satellites are known. Although the radii have been determined many times by a variety of techniques, the results remain somewhat uncertain.

Camichel (1953) measured the diameters of the satellites by comparing them with artificial disks projected in the field of a telescope. The disks were of adjustable size, brightness, color, and limb darkening. Dollfus (1954) also measured the diameters with a double-image micrometer. The two sets of measurements agree around the following values: Jupiter I, 3550 km; Jupiter II, 3100 km; Jupiter III, 5600 km; and Jupiter IV, 5050 km.

Interferometric measurements of the diameters of the satellites have been made by Michelson (1891a, b), who used a double-slit device in front of the objective of a 12-in. refracting telescope. These observations were repeated by Hamy (1899), who used a similar technique, but with larger slits to increase the luminosity of the image. Measurements have also been made by Danjon (1936), who used a half-wave interference micrometer. Systematic differences appear between the diameters obtained by each observer. Diameters measured by Danjon are systematically smaller than those measured by Hamy and Michelson; those obtained by Hamy are systematically smaller than those obtained by Michelson. Danjon (1944) used an improved reduction technique to discuss these interferometric measurements, and succeeded in reconciling them to an accuracy of approximately ± 5 percent. Basic assumptions in his analysis were that each satellite is circular and that its disk is uniformly reflective. His analysis gave the following mean diameters for the satellites: Jupiter I, 3300 km; Jupiter II, 2900 km; Jupiter III, 4400 km; and Jupiter IV, 3900 km.

Filar micrometric measurements of the diameters of the satellites have been made by many observers. In particular, Barnard (1895) used the Lick 36-in. refractor to make an excellent set of measurements. He obtained the following values for the diameters: Jupiter I, 3946 ± 60 km; Jupiter II, 3291 ± 82 km; Jupiter III, 5726 $\pm$ 87 km; and Jupiter IV, 5383 ± 56 km. Barnard compared his results with the mean values obtained from 9 sets of similar observations made by 9 different observers. His results agree closely with those values. Further measurements by Dyson (1895) agree closely with the results obtained by Barnard.

It is by no means clear which of the various techniques for obtaining the diameters of the satellites gives the most accurate results. Perhaps the most useful values are those obtained by straight averaging of the diameters derived from each of the several techniques. The straight mean diameters are: Jupiter I, 3599 ± 326 km; Jupiter II, 3097 ± 196 km; Jupiter III, 5242 ± 733 km; and Jupiter IV, 4778 ± 778 km. The error quoted is the standard deviation. These errors should give a realistic estimate of the uncertainty of the diameters of the satellites. The diameters of satellites I and II appear to be known to an accuracy of ± 5 to 10 percent; the diameter of satellites III and IV appear to be known to rather less accuracy, ± 15 to 20 percent. It will be assumed in the subsequent discussion that the diameters are uncertain by up to ± 20 percent.

Figure 4.9 shows the ingress light curve for the mean satellite and the standard Jovian atmosphere at a wavelength of 5500Å for various adopted values for the radius R of the satellite. Curve 4 refers to the case where the radius is set equal to 2010 km, which is the value listed in Table 2.3 and denoted R_M for convenience. Curve 1 refers to the case of a point satellite, with R set equal to 1 cm. Curves 2 and 6 refer to the cases where R is set equal to 0.5 R_M and 1.5 R_M respectively. Curves 3 and 5 refer to the cases where R is set equal to 0.8 R_M and 1.2 R_M, respectively. If R_M should be uncertain by up to ±20 percent, the calculated light curve would lie between curves 3 and 5.

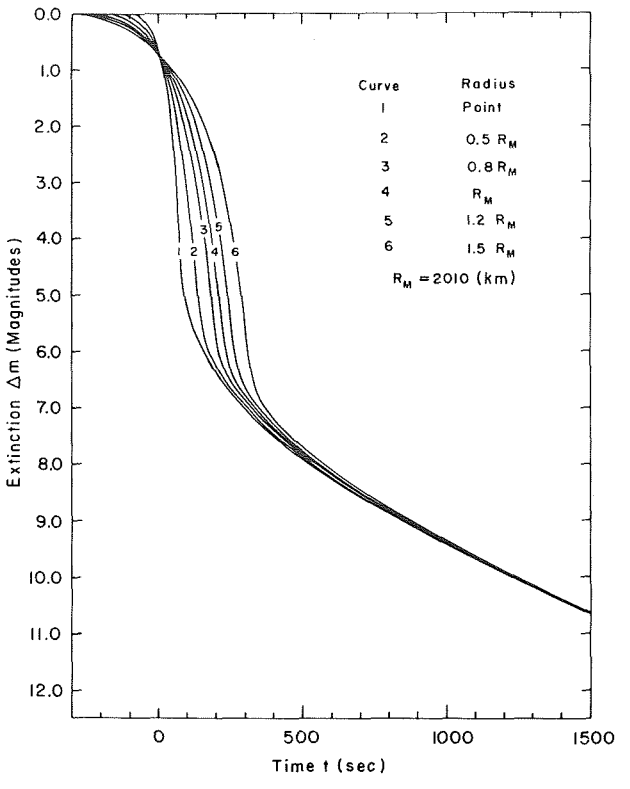

Figure 4.9—The sensitivity of the ingress light curve for the mean satellite to the adopted value for its radius. Standard Jovian atmosphere assumed: λ 5500Å. Radius varied around the best value R_M by up to ±50 percent. Light curve for a point satellite also plotted.

The brighter region of the light curve is far more sensitive to changes in the adopted radius of the satellite than the refraction tail. This behavior of the light curve is a direct consequence of the character of the edge of the Jovian shadow, depicted by curve 2 in Figure 4.2, and the averaging effect of the finite disk of the satellite. Figure 4.9 shows that the refraction tail is very insensitive to changes in the radius of the satellite for extinctions greater than 7 magnitudes. It is clear from Figure 4.9 that the physical properties of the Jovian atmosphere can be very reliably inferred from the refraction tail, even though the radius of the satellite is uncertain by up to 20 percent. It is also clear that the uncertainty in the radius limits the accuracy required in the photometric determination of the shape and location of the refraction tail. If the radius of the satellite is uncertain by ±20 percent, it is unnecessary to measure the brightness of the satellite while on the refraction tail to better accuracy than ±0.1 magnitudes.

G. Effect of Arbitrary Distributions of Reflectivity Over the Disks of the Satellites

In reality, we cannot expect the distribution of reflectivity over the disk of a satellite to be perfectly uniform. We need mention only the case of the Moon, as viewed from Earth with the naked eye, to show how much the distribution may depart from uniformity. To study the sensitivity of the ingress light curve to the distribution of reflectivity over the disk of a satellite, several artificial and rather extreme situations have been studied. Figure 4.10 shows the ingress light curve for the mean satellite and the standard model of the Jovian atmosphere, at a wavelength of 5500Å, for various

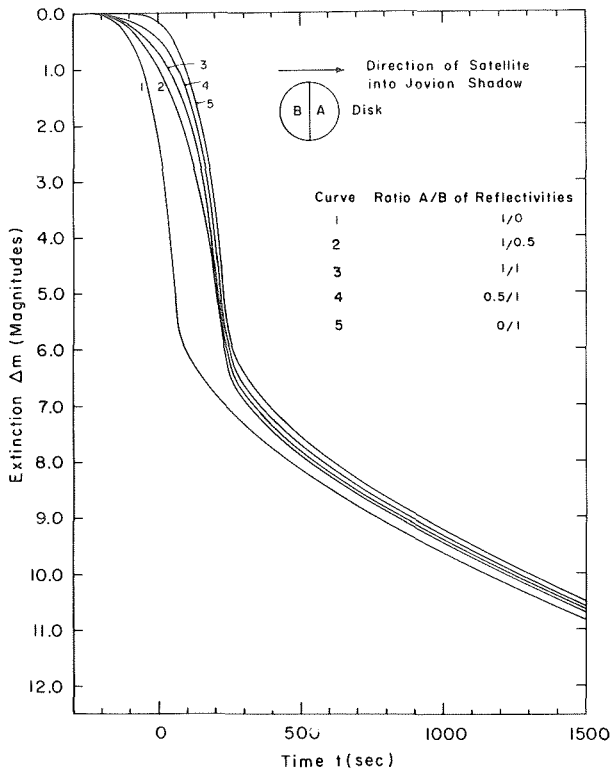

Figure 4.10—The effect on the ingress light curve for the mean satellite of arbitrary and extreme distributions of reflectivity over its disk. Standard Jovian atmosphere assumed: λ 5500Å.

adopted distributions of reflectivity. Curves 1 and 5 both refer to situations where one hemisphere of the satellite is painted uniformly black (zero reflectivity), while the other is painted uniformly white (unit reflectivity). To produce the maximum effect on the light curve, we assume that the line of demarcation between the two hemispheres bisects the disk of the satellite and is oriented tangent to the reference edge of the Jovian shadow at the point of ingress. Curve 1 refers to the case where the white section of the disk precedes the black section into eclipse. Curve 5 refers to the case where the black section enters eclipse first. Two other less extreme situations have also been considered. Their corresponding light curves are shown as curves 2 and 4. In both cases one hemisphere of the satellite is again painted white, but the other hemisphere is a uniform grey instead of being perfectly black. The reflectivity per unit area of the grey hemisphere is one half that for the white hemisphere. Curve 2 refers to the case where the white section of the disk precedes the grey section into eclipse. Curve 4 refers to the case where the grey section enters eclipse first. Curve 3 refers to the idealized case of a uniformly white distribution of reflectivity over the disk. As Harris (1961) first pointed out, the effect on the light curve of changing the distribution of reflectivity over the disk of the satellite is similar to the effect produced by changing its radius. Consequently, the brighter section of the light curve is again sensitive to the physical properties of the satellite. However, the refraction tail is insensitive to the distribution of reflectivity over the disk, even for the extremely artificial cases that have been considered. Such extreme cases are, of course, very unlikely to occur in nature. In fact, dark and bright regions are expected to be fairly evenly distributed over the surface of the satellite. Such a distribution would cause the average reflectivities of both hemispheres to be more nearly equal. Evidence does exist to show that dark and bright regions are indeed fairly evenly distributed over the surfaces of the Galilean satellites. Maps of their surfaces, based on visual observations made by Lyot, Camichel, and Gentili at the Pic du Midi Observatory, have been published by Dollfus (1961). Besides depicting the coarse surface features of the satellites, the observations showed that each satellite's period of rotation was equal to its period of revolution around Jupiter. It is fortunate that a detailed knowledge of the distribution of reflectivity over the disks of the satellites is not essential. It has been pointed out that the physical properties of

the Jovian atmosphere can be reliably studied using photometric observations of the refraction tails of the ingress light curves accurate to no better than ± 0.1 magnitudes. Only if the observations are made to greater accuracy need the assumption that the disks of the satellites are uniformly reflective be abandoned.

H. Limits Imposed by Critical Refraction

If the level at which critical refraction occurs in the Jovian atmosphere is below the cloud tops, the location of the cutoff region on the refraction tail of the ingress light curve, for each of the Galilean satellites, will be determined by the pressure at the cloud tops. If the critical refraction level occurs above the clouds, the refraction tail will be prematurely truncated. If the standard model should adequately describe the atmosphere, the height above the clouds, at which horizontal rays of light of wavelength 5500Å are critically refracted, would be 19.2 km, corresponding to a pressure level of 5.1×10^5 dyne/cm^2. The eclipse technique for scanning the physical structure of the atmosphere in height could not, therefore, be used to study the region below a height of about 20 km above the clouds. There are, however, reasons for believing that the standard model may be inappropriate. In particular, the adopted value for the scale height may be too small. A larger value would cause a reduction in the adopted pressure at the cloud tops. In addition, it would increase the value of the refractivity required to produce critical refraction. Both effects would reduce the height above the cloud tops at which critical refraction would occur. It is even possible that critical refraction might occur within the clouds, in which case the entire region of the atmosphere above the clouds could be scanned by the eclipse technique.

Critical refraction will severely limit the effectiveness of a radio beam occultation experiment performed using a spacecraft flyby of the planet. The experiment cannot be used to scan the deeper regions of the Jovian atmosphere because the level of critical refraction for S-band radiation occurs relatively high in the atmosphere. In fact, critical refraction occurs for both S-band and optical radiation at very nearly the same level, because refractivity changes only slowly with wavelength. Since refractivity decreases with increasing wavelength, the critical refraction level for S-band radiation will be slightly lower than the corresponding level for optical radiation. The eclipse technique for studying the physical structure of the Jovian atmosphere can, therefore, compete very favorably with the radio beam occultation experiment.

CHAPTER 5

OBSERVATIONAL CONSIDERATIONS

A. Geometrical Problems

The main geometrical problem is the ability of an observer on Earth to view the satellite clearly as it enters the edge of the Jovian shadow. The optimum geometrical conditions for observing one of the Galilean satellites at ingress occur when Jupiter is at quadrature before opposition. The optimum geometry is shown in Figure 5.1. At that time the phase angle of Jupiter will be at its maximum value of approximately 11°, and each of the satellites will pass into eclipse at the greatest possible angular distance from the Jovian limb. Under the geometrical assumptions made in Chapter 2 of this paper the maximum distances from the Jovian limb at which the Galilean satellites enter eclipse are, in terms of the apparent radius of Jupiter as unity: Jupiter I, 1.2; Jupiter II, 1.8; Jupiter III, 2.9; and Jupiter IV, 5.0. To convert these distances into seconds of arc, note that near opposition the apparent angular radius of Jupiter is approximately 21" of arc.

Observations of the ingress light curves of the Galilean satellites are possible for several months both before and after Jupiter reaches quadrature before opposition. Observations may be started, in principle, fairly soon after solar conjunction and several months before quadrature. However, certain observational problems occur that are related to the geometrical situation. First, the changing proximity of the satellite at ingress to the limb of the planet plays a role in determining the width in time of the useful observational window. Second, the distance between Jupiter and the Earth is significantly larger before quadrature than after, with the consequence that the satellite appears fainter before quadrature and photometric measurements are correspondingly more difficult to obtain. Third, the proximity of the

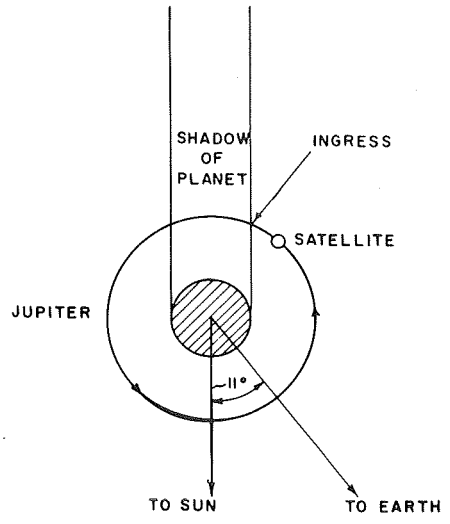

Figure 5.1—The optimum geometry for the observation from Earth of the ingress light curve for the mean satellite. Jupiter is at the quadrature point before opposition. Orbits of Earth and Jupiter around the Sun are assumed to be coplanar. Plane of orbit of the satellite around Jupiter contains the line of sight for an observer on Earth. The diagram is not to scale.

Sun to the planet also limits the width of the observational window. Observations are easiest between quadrature and opposition for several reasons: the angular separation of Jupiter and the Sun is larger than between solar conjunction and quadrature; and the satellites appear brighter because the distance between Jupiter and the observer has steadily decreased. Observations cannot, however, be continued right up to the date of opposition because photometric problems become increasingly severe as the satellites enter eclipse closer to the limb of the planet. To summarize, observations are feasible for approximately 3 months per year. The window extends from about 6 weeks before quadrature before opposition to about 6 weeks after.

B. Photometric Problems

Diffuse Radiation Multiply Scattered from the Jovian Atmosphere

Mention was made earlier of the illumination of the Galilean satellites, while in the Jovian shadow, by the bright ring that appears to surround the planet when viewed from within its shadow. The ring is produced by multiple scattering of sunlight in the Jovian atmosphere above the cloud tops. During ingress the illumination of the satellite by the bright ring is negligible compared with the illumination by the refracted solar disk, as will now be shown.

Consider first the illumination of the mean satellite outside eclipse. Let the solar flux at the mean distance of Jupiter from the Sun, and at a visual wavelength of 5500Å, be N_P photons/cm^2/sec/Å. The number of such visual solar photons directly incident per second per unit angstrom on the satellite just before ingress will be

$$\pi R_s^2 N_p , \tag{5.1}$$

where R_S is the radius of the satellite.

Consider next the illumination of the mean satellite at the center of the Jovian shadow. By the time the satellite reaches this region of the shadow, the refracted solar disk will have long since been occulted by the planet and will no longer be visible to an observer on the satellite. The satellite will then be illuminated only by the solar photons which have been diffusely scattered in the Jovian atmosphere above the clouds. Suppose that the atmospheric ring has an effective thickness ΔX. The number of solar photons incident per second per unit angstrom directly on the ring will be

$$2\pi R_J \Delta X N_p , \tag{5.2}$$

where R_J is the radius of Jupiter. If it is assumed that the atmospheric ring scatters this radiation isotropically, the fraction of these photons which reach the satellite will be

$$\frac{\pi R_s^2}{4\pi r_s^2} \tag{5.3}$$

or, more simply,

$$\frac{R_s^2}{4r_s^2}, \tag{5.4}$$

where r_S is the radius of the orbit of the satellite around the planet.

The effective scattering atmosphere may be assumed to be optically fairly thin, extending downward for approximately one scale height from the level at which the optical length along a ray path tangent to the limb of the planet reaches unity. Above that level the probability of scattering rapidly approaches zero as the number density decreases with height. Deeper than one scale height below that level, the probability of a photon passing through the atmosphere by multiple scattering is very small because of the rapid increase in the optical thickness. For the adopted standard model of the Jovian atmosphere ΔX is 8.3 km.

The ratio of the brightness of the satellite outside eclipse to its brightness when illuminated only by scattered radiation from the atmospheric ring is

$$\frac{\pi R_s^2 N_p}{2\pi R_J \Delta X N_p \left(\frac{\pi R_s^2}{4\pi r_s^2}\right)} \tag{5.5}$$

or, more simply,

$$\frac{2r_s^2}{R_J \Delta X}, \tag{5.6}$$

which is numerically equal to 3.45×10^6. It follows that when the satellite is illuminated only by the ring it will be 16.3 magnitudes fainter than outside eclipse. Therefore, illumination by the atmospheric ring has a negligible effect on the ingress light curves for the Galilean satellites for extinctions of less than about 12.5 magnitudes.

Accurate Measurement of Satellite Brightness at Low Light Levels

General Remarks: Introduction to the Area-Scanning Technique

As mentioned in Chapter 1, the most thorough observational work on the photometry of the ingress light curves of the Galilean satellites was carried out many years ago by Kuiper and Harris. Their observations have been discussed in detail by Harris (1961). It is clear from his discussion that it is extremely difficult to make useful observations of the refraction tails of the light curves with conventional photoelectric photometers because of scattered light from the nearby bright planetary disk. Kuiper and Harris used the 82-in.-aperture McDonald reflector fitted with a conventional photoelectric photometer which had a circular diaphragm of 12" of arc aperture. Because the apparent angular diameters of the Galilean satellites are approximately 2" of arc, a large aperture diaphragm was used to avoid possible vignetting of the image introduced by guidance problems, even after the drive rate of the telescope had been corrected for the drifts introduced by motion of the planet with respect to the stars, motion of the satellite with respect to the planet, and changes in the refraction in the terrestrial atmosphere. In principle, a smaller diaphragm, with perhaps a diameter of 4" of arc, could have

been used if the periodic errors in the drive screw were less than about 1" of arc. Diaphragms with diameters less than about 4" of arc would not have been feasible because of variation in the diameter of the seeing disk of up to about 1" of arc. Kuiper and Harris took no special precautions to minimize scattered light from the nearby planet in the optical system of the telescope. Consequently, they found that even if each of the satellites was observed near quadrature before opposition, accurate measurements of their ingress light curves could not be made fainter than an extinction of about 6 or 7 magnitudes. In addition, they found that the satellites became undetectable against the bright sky background for an extinction of about 9 magnitudes. Below that level the signal from the satellite disappeared in the noise of the bright background. The observations were made through a wide-band yellow filter; Kuiper's earlier visual observations had shown that the eye could follow the satellite to about the same limit. The limiting magnitude for the visual observations against the bright background was roughly estimated as 14.5.

The experience of Kuiper and Harris suggests that even a relatively minor improvement in photometric technique should allow accurate photometric observations of the refraction tails of the light curves to be made. The problem is how to detect and accurately measure a faint signal against a bright background. Because conventional astronomical photometers are not designed for this type of measurement, a new technique must be used. A partial breakthrough was achieved by Rakos (1965, 1966) who successfully developed an area-scanning photometer. The advantage of area scanning is that, by integrating many scans, the faint signal appears above the noise of the bright background. As the integration proceeds, the noise level of the sky decreases while the faint signal is accentuated. Very soon the signal appears well above the noise level and may be accurately measured. Rakos developed the scanning technique specifically to observe eclipses of Phobos by Mars. His objective was to infer the physical properties of the Martian atmosphere from the ingress light curve. The observational problem he encountered was much more difficult than our own. He had to make observations of Phobos when it was only 4" of arc from the bright limb of Mars and when the magnitude difference between planet and satellite, before ingress, was 13. In the case of the Galilean satellites entering eclipse, observations may be made some tens of seconds of arc from the bright limb at quadrature before opposition. At such great distances from the bright limb, the sky brightness is much less than it is when close to the planet. In addition, the magnitude difference between planet and satellite, before ingress, is only about 8. The scattered light problem is, therefore, far less severe.

In the operation of the Rakos photometer, a small region of the sky is optically scanned, by means of a rocking mirror technique, through a narrow slit situated in front of a Fabry lens/photomultiplier system. In this manner a rectangular strip of sky, with dimensions of perhaps 4" x 10", depending on the scale in seconds of arc per millimeter at the slit of the photometer, may be repeatedly scanned. Appreciable changes in the seeing do not normally occur in a clear sky over such a small area in less than ~ 0.1 sec, which is the time required to complete each scan. Individual scans are displayed on an oscilloscope and then recorded on film. Averages are then taken of groups of 100 consecutive scans, to reduce the statistical fluctuations of the individual scans.

However, because the averaging must be done by hand, it is unavoidably subjective. The area-scanning photometric technique has been developed further since the pioneering work done by Rakos. Very recently Hall (1968) constructed a twin-beam area-scanning polarimeter. He greatly improved the efficiency and sensitivity of the area-scanning technique by automatically carrying out the integration of the individual scans at the telescope, while the observations were actually in progress. Each of the beams of light in the polarimeter was fed to a separate photomultiplier and amplifier. The photometric data were then fed into two multichannel analyzers that integrated the individual scans. The averaged scan obtained during each integration period was punched on tape and later reduced by computer. The Hall photometer is ideally suited to the measurement of the refraction tails of the ingress light curves of the Galilean satellites. It will be shown that the necessary observations may be made with this photometer attached to a telescope of only moderate size, e.g., only 72-in. aperture.

Observational Technique

Ideally, the telescope should accurately track the satellite as it enters the Jovian shadow. Allowances should be made for the motion of the satellite with respect to Jupiter, in addition to the motion of Jupiter with respect to the stars and the drift produced by variation in the refraction in the terrestrial atmosphere during the course of the observations. However, it may not be possible to guide the telescope on the satellite itself when ingress has progressed to the point where the satellite's disk is being illuminated only by refracted solar radiation. The satellite may then be too faint to be seen easily. The telescope should, therefore, be guided by an offset technique on the limb of Jupiter from the very start of ingress.

The rectangular area of the sky that is scanned by the photometer should be oriented in one of several ways, depending on whether the telescope is tracking on the satellite itself or on Jupiter. In the ideal case, when the telescope is accurately tracking on the satellite, the scanned area should be radially oriented to the planet because the brightness of the sky background is a function only of the radial distance from the center of the planetary disk. Radial orientation would permit the scattered light to be very accurately subtracted from the signal from the satellite itself. When the telescope is guided on the limb of Jupiter, the scanned area should be oriented so that the apparent direction of motion of the satellite, with respect to the planet, is exactly along the greatest length of the rectangle.

Care must be exercised in choosing both the dimensions of the scanned area and the width of the slit of the scanner. The area scanned should be about 4" of arc wide and about 10" of arc long. The width of the rectangle should be kept as small as possible, to keep the scattered light level to a minimum. A slit length of 4" of arc will allow for fluctuations in the seeing of an order of 1" of arc or less, and will permit small errors to be made in the orientation of the scanned area. The slit should be no wider than about 0".2, to permit the disk of the satellite to be adequately resolved. Resolution of the satellite is desired to maximize the signal/sky ratio.

A time resolution of between 10 and 20 sec should be selected so that the precise shape of the ingress light curve can be obtained for each of the satellites. During the course of the integration period, it is desirable that the satellite not change its position in the scanned area by any appreciable amount. If it does, the reason for making the integration is lost. When the telescope is accurately tracking the satellite there is no problem. When the telescope is tracking on the limb of the planet, the motion of the satellite with respect to the scanned area in a 10-sec period will typically be less than 0".1, a very small fraction of the apparent diameter of the satellite.

Use of the Hall photometer will enable all these observational problems to be overcome very simply. The photometer is fitted with an offset guider. It will be a simple matter, therefore, to guide the telescope on the limb of the planet. At ingress, the drift direction of the satellite, with respect to the planet, will be closely parallel to the Jovian equator. Orientation of the scanned area will, therefore, be simple because the satellite will drift parallel to the dark belts visible on the disk of the planet. The scanned area can be easily located so that during ingress the satellite moves along the length of the rectangle from one end to the other. To orient the scanned area, the whole photometer may be easily and accurately rotated around the optical axis of the telescope.

Photon Statistics and Telescope Aperture

In the application of an area-scanning photometer to the accurate measurement of the refraction tails of the ingress light curves of the Galilean satellites, the length of the area scanned is divided into a large number of channels, perhaps 100 or more. As the area is scanned, photoelectron counts are recorded in each of these channels and integrated over many scans, using a multichannel analyzer. A typical record from the multichannel analyzer at the end of an integration period is shown in Figure 5.2. As indicated earlier, the signal is accentuated relative to the noise of the sky background. The noise of the background is reduced as the number of counts increases. It is important to understand that the noise results merely from statistical fluctuations in the relatively small number of photons counted. If both the sky transparency and seeing conditions are good, it can be assumed that the brightness of a particular point in the sky is constant to within 1 percent for a period of up to an hour or so.

With reference to Figure 5.2, the area under the signal spike and above the sky background is linearly related to the brightness of the satellite. It is necessary to know how accurately that area can be determined so that the uncertainty of the measurement of the satellite brightness may be reliably estimated. The area is proportional to the total number of counts recorded above the sky background, when photons from the disk of the satellite are passing through the slit of the area scanner. To discuss the statistics of photon counting, certain parameters must be defined. Let the length of the slit of the area scanner be Δw; the width of the slit of the area scanner be Δl; the total length of the area of sky scanned be l; the duration in time of each scan be Δt; the total number of scans in each integration period be N; the integration period be T; the flux of photons per cm^2 per sec, integrated over the bandwidth of the chosen filter and arriving at the top of the atmosphere from the satellite, be N_{sat}; the corresponding flux of photons,

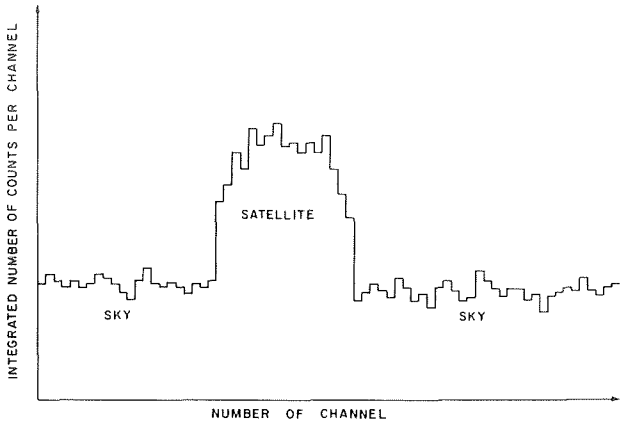

Figure 5.2—A typical record from the multichannel analyzer at the end of an integration period.

apparently from each square second of arc of sky near the satellite, be N_{sky}; the angular diameter of the satellite be d sec of arc; the ratio of the brightness of the satellite to the brightness of a neighboring region of sky of equal width d, but of area $(d.\,\Delta w)$, be R; the efficiency of the observational system in converting photons incident on the top of the atmosphere into photoelectrons in the photomultiplier (counts) be f; the diameter of the aperture of the telescope be D; the number of photoelectrons counted per scan, when light from the satellite is passing through the slit of the area scanner, be $(n_{sig} + n_{sky})$; and the number of photoelectrons counted per scan, when light from an equivalent width d of neighboring sky is passing through the slit of the area scanner, be n_{sky}.

For a given set of equipment the accuracy of the measurements is dependent primarily on the selected period of integration. The relation between T, N, and Δt is given by

$$T = N\,\Delta t\,. \tag{5.7}$$

Clearly, we may write

$$n_{sig} = N_{sat}\frac{\pi D^2}{4} f\left(\Delta t \frac{d}{l}\right) \tag{5.8}$$

and

$$n_{sky} = (N_{sky}\, d\, \Delta w)\frac{\pi D^2}{4} f\left(\Delta t \frac{d}{l}\right). \tag{5.9}$$

The basic signal/sky ratio, R, is given by

$$R = \frac{n_{sig}}{n_{sky}} = \frac{N_{sat}}{N_{sky}\, d\, \Delta w}\,. \tag{5.10}$$

Obviously to optimize the signal/sky ratio, the area of sky being sampled simultaneously with the satellite must be as nearly equal to the area of its disk as possible. Since Δw has been selected to be close to $2d$ to ease the guidance problem during the observations, the area of sky being sampled is rather more than twice the area of the satellite.

There are three basic statistical problems involved in the accurate determination of the brightness of the satellite. The first is concerned with the accurate measurement of the integrated signal from the satellite alone. To study this problem, it can be

assumed for simplicity that the brightness of the sky background is zero. After N scans, the integrated count for the satellite is Nn_{sig}. By elementary statistics the uncertainty in the count is $\pm\sqrt{Nn_{sig}}$. The percentage of accuracy in the determination of the brightness of the satellite will be $100/\sqrt{Nn_{sig}}$.

The second problem is concerned with the accurate measurement of the integrated signal from the satellite against the sky background. For simplicity, it can be assumed that the integrated count for the satellite alone, Nn_{sig}, is known with infinite accuracy. After N scans, the integrated count for the sky Nn_{sky}, will be known with an accuracy of $\pm\sqrt{Nn_{sky}}$. We may define the parameter R_1 to be the ratio of the integrated signal from the satellite alone to the noise level of the integrated sky count. Therefore,

$$R_1 = \frac{Nn_{sig}}{\sqrt{Nn_{sky}}} \tag{5.11}$$

or

$$R_1 = \sqrt{Nn_{sky}}\, R. \tag{5.12}$$

The third problem is to determine the minimum brightness of the satellite when it is still just detectable against the noise of the sky background. The parameter R_2 can be defined as the minimum value of R that is detectable with the particular observational system being used. For the signal from the satellite to appear above the noise level of the sky after integration over N scans, it is required that

$$Nn_{sig} > \sqrt{Nn_{sky}} \tag{5.13}$$

or

$$R > \frac{1}{\sqrt{Nn_{sky}}}. \tag{5.14}$$

It follows that

$$R_2 = \frac{1}{\sqrt{Nn_{sky}}}. \tag{5.15}$$

To demonstrate the feasibility of accurately measuring the ingress light curves to low light levels at visual wavelengths with a telescope of only moderate size, the use of the Hall twin-beam photometer attached to a 72-in. Cassegrain reflecting telescope will be considered. Assume that the telescope is located at Flagstaff, Arizona. Observations of the light curves, in two colors simultaneously, may be made provided certain minor modifications of the photometer are carried out. In particular, it is necessary to restrict the length of the area scanned by changing an appropriate cam in the photometer. To facilitate detection of the satellite against the sky background, the integration period should be 20 seconds to allow 20 scans to be made at the rate of one

per second. A longer integration period will distort the observed shapes of the ingress light curves. If the refraction tails of the light curves are to be well defined, accurate photometric measurements of each satellite must be made when it has suffered up to 10 magnitudes extinction. At that level of extinction, it is necessary to determine the brightness of the satellite to an accuracy of 10 percent or better.

It will be assumed that observations are made using the V-filter, which corresponds to an effective wavelength of 5500Å, and that the dimensions of the area scanned are restricted to 4" × 10". The collecting area of the primary mirror of the telescope (D = 72 in.) is 2.62×10^4 cm^2. The efficiency of the observational system is the product of the efficiencies of its individual components, which are as follows:

(a) Typical transmission efficiency of clear atmosphere = 0.7 (altitude of Flagstaff, 2210 meters; elevation of Jupiter > 30° above horizon, i.e., atmospheric path < 2 air masses). The transmission efficiency is derived from Allen (1963) who gives "V-absorption for a clear atmosphere = 0.20 mag/air mass."

(b) Efficiency of Cassegrain telescope (2 mirrors; aluminum coatings) = $(0.8)^2$ = 0.64.

(c) Efficiency of Hall photometer (each beam):

4 optical components = $(0.8)^4$ = 0.41,
Wollaston prism beam-splitter = 0.5,
V-filter = 0.5,
Photocathode = 0.1.

It follows that the efficiency of the observational system is $0.7 \times 0.64 \times 0.41 \times 0.5 \times 0.1 \times 0.5 = 0.0046 \approx 0.5\%$.

Consider next the fluxes of satellite and sky photons within the V-filter bandwidth which strike the top of the atmosphere before and during ingress. From Table 2.3, the apparent magnitude of the mean satellite just before ingress will be $m_v = +5.54$. The apparent magnitude at 10 magnitudes extinction will be $m_v = +15.54$. From the experiences of Kuiper, Harris, and the author, in attempting to carry out photoelectric photometry of the refraction tails of the ingress light curves when Jupiter nears quadrature before opposition, the brightness of an area of background sky equal in area to the disk of the satellite, typically should correspond to an apparent magnitude $m_v = +14.5$. Of course, if the aluminum surfaces of the mirrors are badly oxidized, dirty, or scratched, the sky brightness will be considerably higher. The flux of radiation, at visual wavelengths outside the Earth's atmosphere, which corresponds to a given apparent stellar magnitude m_v, may be obtained from the formula given by Allen (1963)

$$\log_{10} f_\lambda = -0.4 m_v - 8.42 , \qquad (5.16)$$

where f_λ is the flux in ergs/cm^2/sec/Å. For $m_v = +5.54$, $\log_{10} f_\lambda = -10.62$, and $f_\lambda = 2.4 \times 10^{-11}$ ergs/cm^2/sec/Å. Let us assume that the equivalent width of the V-filter is 500Å. The flux F_v integrated over the width of the V-filter is, therefore, equal to 1.2×10^{-8} ergs/cm^2/sec. The energy of a photon of wavelength 5500Å is equal to 3.6×10^{-12} ergs.

If N_v is the number of photons striking the top of the atmosphere in the V-filter bandwidth/cm^2/sec, then

$$N_v = 3.3 \times 10^3 \text{ photons/cm}^2\text{/sec, for } m_v = +5.54 ,$$

$$N_v = 0.33 \text{ photons/cm}^2\text{/sec, for } m_v = +15.54 , \tag{5.17}$$

and

$$N_v = 0.83 \text{ photons/cm}^2\text{/sec, for } m_v = +14.5 .$$

For the mean satellite at an extinction of 10 magnitudes, it follows from Equation 5.8 that

$$n_{sig} = 0.33 \times 2.62 \times 10^4 \times 0.005 \times (1 \times 2/10) \tag{5.18}$$

or

$$n_{sig} = 8.6 \text{ counts/scan,} \tag{5.19}$$

for a scan rate of one per second. Similarly,

$$n_{sky} = (2 \times 0.83) \times 2.62 \times 10^4 \times 0.005 \times (1 \times 2/10) \tag{5.20}$$

or

$$n_{sky} = 43.2 \text{ counts/scan.} \tag{5.21}$$

In Equation 5.20 the number of photons corresponding to the sky background has been increased by a factor of 2, because the area scanned has a width twice the diameter of the satellite.

From Equation 5.19, the accuracy of the measurement of the signal from the satellite, at 10 magnitudes extinction, will be 13.1 percent for an integration period of 20 seconds. From Equation 5.10 the parameter R for 10 magnitudes extinction is 0.2. It follows from Equations 5.12 and 5.21 that R_1 is equal to 5.9. The accuracy of the measurement of the integrated signal, from the satellite against the sky background, will be about 17 percent. The apparent magnitude of the satellite, when it becomes no longer detectable, may be estimated from Equations 5.15 and 5.21. Thus, R_2 is equal to 0.034, which corresponds to an apparent magnitude for the satellite of about 18, i.e., 12.5 magnitudes extinction.

It should be borne in mind that the estimates of background sky brightness, efficiency of the observational system, and bandwidth of the filter, have been deliberately chosen to be conservative. It can be concluded, therefore, that valuable observations of the refraction tails of the ingress light curves of the Galilean satellites can be made with area-scanning photometers of the type developed by Hall attached to telescopes of only moderate size.

CHAPTER 6

CONCLUDING REMARKS

A radio beam occultation experiment performed during a spacecraft flyby mission to Jupiter is not the most efficient technique available for studying the physical structure of the Jovian atmosphere. This paper has described in detail how eclipses of the Galilean satellites may be utilized to give a simple, inexpensive, yet extremely powerful method of thoroughly monitoring the physical properties of the Jovian atmosphere above the visible cloud layer. The relevant observational data may be obtained with telescopes of only moderate size coupled with relatively simple photometers. It appears that much of the data required for a complete understanding of the physical structure of the Jovian atmosphere may be obtained without the use of spacecraft, but from available ground-based astronomical facilities.

Goddard Space Flight Center
National Aeronautics and Space Administration
Greenbelt, Maryland, December 15, 1969
039-52-01-01-51

REFERENCES

Allen, C. W., "Astrophysical Quantities," Second Edition, London: Athlone Press, London, 1963.

Barnard, E. E., Mon. Not. Roy. Astron. Soc. 55: 382, 1895.

Baum, W. A., and Code, A. D., Astron. J. 58: 108, 1953.

Biswas, S., and Fichtel, C. E., Space Sci. Rev. 4: 709, 1965.

Camichel, M., Ann. Astrophys. 16: 41, 1953

Danjon, A., Ann. Observ. Strasbourg III-4: 181, 1936.

Danjon, A., Ann. Astrophys. 7: 135, 1944.

Dollfus, A., C. R. H. Acad. Scie. 238, 1475, 1954.

Dollfus, A., "Planets and Satellites," Volume 3, Edited by G. P. Kuiper and B. M. Middlehurst, Chigago: University of Chicago Press, Plate 40, pp. 554-555, 1961.

Dyson, F., Mon. Not. Roy. Astron. Soc. 55: 477, 1895.

Erdélyi, A., "Higher Transcendental Functions," Volume 1, Batemann Manuscript Project, California Institute of Technology, New York: McGraw-Hill Book Co., Inc., 1953.

Fabry, Ch., J. Observateurs 12: 1, 1929.

Fink, U., and Belton, M. J. S., J. Atm. Sciences 26: 952, 1969.

Hall, J. S., Lowell Observ. Bull. 143, 1968.

Hamy, M., Bull. Astron. 16: 257, 1899.

Harris, D. L., "Planets and Satellites," Volume 3, Edited by G. P. Kuiper and B. M. Middlehurst, Chicago: University of Chicago Press, pp. 327 et seq., 1961.

Hunten, D. M., and McElroy, M. B., J. Geophys. Res. 73: 4446, 1968.

Kuiper, G. P., Astron. J. 52: 147, 1947.

Melbourne, W. G., Mulholland, J. D., Sjogren, W. L., and Sturms, F. M., Jr., NASA Technical Report 32-1306, 1968.

Michelson, A. A., Pub. Astron. Soc. Pacific 3: 274, 1891.

Michelson, A. A., Nature 45: 160, 1891.

Owen, T., and Mason, H. P., Astrophys. J. 154: 317, 1968.

Pannekoek, A., Astron. Nachr. 164: 5, 1903.

Rakos, K. D., Appl. Opt. 4: 1453, 1965.

Rakos, K. D., Lowell Observ. Bull. 131, 1966.

Watson, G. N., "A Treatise on the Theory of Bessel Functions," New York: Cambridge University Press, 1958.

NASA-Langley, 1970 —— 30

"The aeronautical and space activities of the United States shall be conducted so as to contribute . . . to the expansion of human knowledge of phenomena in the atmosphere and space. The Administration shall provide for the widest practicable and appropriate dissemination of information concerning its activities and the results thereof."

—NATIONAL AERONAUTICS AND SPACE ACT OF 1958

NASA SCIENTIFIC AND TECHNICAL PUBLICATIONS

TECHNICAL REPORTS: Scientific and technical information considered important, complete, and a lasting contribution to existing knowledge.

TECHNICAL NOTES: Information less broad in scope but nevertheless of importance as a contribution to existing knowledge.

TECHNICAL MEMORANDUMS: Information receiving limited distribution because of preliminary data, security classification, or other reasons.

CONTRACTOR REPORTS: Scientific and technical information generated under a NASA contract or grant and considered an important contribution to existing knowledge.

TECHNICAL TRANSLATIONS: Information published in a foreign language considered to merit NASA distribution in English.

SPECIAL PUBLICATIONS: Information derived from or of value to NASA activities. Publications include conference proceedings, monographs, data compilations, handbooks, sourcebooks, and special bibliographies.

TECHNOLOGY UTILIZATION PUBLICATIONS: Information on technology used by NASA that may be of particular interest in commercial and other non-aerospace applications. Publications include Tech Briefs, Technology Utilization Reports and Notes, and Technology Surveys.

Details on the availability of these publications may be obtained from:

SCIENTIFIC AND TECHNICAL INFORMATION DIVISION

NATIONAL AERONAUTICS AND SPACE ADMINISTRATION

Washington, D.C. 20546